# Mechanical Effects of Electrodes on the Vibrations of Quartz Crystal Plates

Peter C. Y. Lee, *Member, IEEE*, and Rui Huang

*Abstract*—**A system of approximate first-order equations is extracted from an infinite system of 2-D equations for piezoelectric crystal plates with thickness-graded material properties, which is deduced from the 3-D equations of linear piezoelectricity. These equations are used to study mechanical effects on the thickness-shear (TS), flexural (F), and face-shear (FS) vibrations of an AT-cut quartz plated with two identical electrodes.**

**Dispersion curves are calculated from the present 2-D equations as well as the 3-D equations. The comparison of these curves shows that the agreement is very close for all three frequency branches of TS, F, and FS modes in a range up to the 1.5 times the fundamental TS frequency and for gold and aluminum electrodes with $R$, the ratio of the mass of the electrodes to that of the plate, equal to 0.05. without introducing any correction factors.**

**In order to assess electrode effects, spectra of $\Omega$ vs. $a/b_q$ (length-to-thickness ratio of the quartz) are computed for plates with gold and aluminum electrodes and different R ratios. And the spectrum of $\Omega$ vs. $R$ is computed for plates with aluminum electrodes and a given $a/b_q$ ratio. For a plate with gold electrodes, the frequencies of predominant TS, F, and FS modes are decreasing as $R$ increases, but the amount of frequency changes for the TS mode is much greater than those for the other two modes. However, for a plate with aluminum electrodes, the frequencies of the TS and FS modes are decreasing, but those of the F modes are increasing as $R$ increases.**

## I. Introduction

A system of five first-order equations of motion for piezoelectric crystal plates with platings was derived by Mindlin [1] in which the resulting equations have the same number and almost the same form as those for the crystal plate alone (by power series expansion), except the coefficients of the elastic stiffness and those of the inertia terms are slightly modified. In the 2-D plate equations derived by trigonometrical series expansion [2], the modification of the inertia terms due to the mass effect of electrodes was similarly obtained. These equations are simple and easy to use, but they are limited to plates with very thin electrodes.

As the resonating structures in the micro-electromechanical systems (MEMS) become smaller and thinner, the ratio of the electrode to the plate thickness becomes significantly larger [3]. In these cases, the mechanical properties of the electrodes (such as the mass density, thickness and elastic stiffness), must be taken into account.

Exact solutions of the 3-D equations for an infinite isotropic plate fully covered by isotropic platings were obtained by Lee and Chang [4]. Similar solutions for an AT-cut quartz plate with identical electrodes are obtained and included in the present paper. Exact analysis of acoustic waves in multilayered piezoelectric plates using the transfer matrix method was presented by Stewart and Yong [5]. These solutions provide the exact dispersion relations (i.e., the frequency-wave number relations for straight-crested waves in an infinite plate), but they cannot be easily extended to those of finite plates.

In the present paper, an infinite system of 2-D equations for piezoelectric crystal plates with thickness-graded material properties is deduced from the 3-D equations of linear piezoelectricity by an approach similar to that of Lee and Yu [6] with the new series expansion of Lee *et al.* [7]. Then, a system of 2-D first-order equations is extracted from the infinite set for the study of the thickness-shear (TS), flexural (F), and face-shear (FS) vibrations of an AT-cut quartz plate with two identical electrodes and a pair of parallel free edges.

We note that the derivation of the present equations is similar, in general, to those of the composite or laminated plate theories, for instance, the laminated plate theory by Yong *et al.* [8]. However, no correction factors are introduced in the present 2-D equations to improve the predicted dispersion relations because of the use of the new series expansion [7].

## II. Two-Dimensional Equations

For a piezoelectric crystal of volume $V$ and bounded by surface $S$, the 3-D equations of linear piezoelectricity are summarized below.

The stress equations of motion and the charge equation of electrostatics and boundary conditions in variational form, which can be obtained from a variational principle [9]:

$$\int_{t_0}^{t} dt \int_V [(T_{ij,i} - \rho \ddot{u}_j)\delta u_j + D_{i,i}\delta\phi]\, dV = 0,$$
$$\int_{t_0}^{t} dt \int_S [(t_j - n_i T_{ij})\delta u_j - (\sigma + n_i D_i)\delta\phi]\, dS = 0. \quad (1)$$

Manuscript received April 17, 2001; accepted December 11, 2001. This work was supported by Grant No. DAAH 04-95-1-0102 from the U.S. Army Research Office.

The authors are with the Department of Civil and Environmental Engineering, Princeton University, Princeton, NJ 08544 (e-mail: lee@princeton.edu).

The constitutive equations:

$$T_{ij} = c_{ijkl}S_{kl} - e_{kij}E_k,$$
$$D_i = e_{ijk}S_{jk} + \epsilon_{ij}E_j. \tag{2}$$

The strain-displacement relations and the electric field-potential relations:

$$S_{ij} = \frac{1}{2}(u_{i,j} + u_{j,i}),$$
$$E_i = -\phi_{,i}. \tag{3}$$

In the above, $T_{ij}$, $S_{ij}$, $u_i$, $D_i$, and $E_i$ are the components of stress, strain, mechanical displacement, electric displacement, and electric field, respectively; and $\phi$ is the electric potential. Material properties are the elastic stiffness coefficients $c_{ijkl}$, the piezoelectric strain constants $e_{ijk}$, the dielectric permittivity $\epsilon_{ij}$, and the mass density $\rho$.

In $(1)_2$, $t_i$ and $\sigma$ are the surface traction and surface charge density, respectively, and $n_i$ is the unit outward normal to the surface $S$. Equation (1) will be used to deduce a system of 2-D equations and associated face and edge conditions for piezoelectric crystal plates.

In [6], 2-D equations for piezoelectric crystal plates with thickness-graded material properties were derived by essentially power series expansion, and they were used to study the vibrations of homogeneous and symmetric bimorph disks in [10] and of asymmetric bimorph disks of piezoelectric ceramics in [11]. Predicted results compare closely with experimental data. However, in these equations, correction factors were introduced to adjust the cut-off frequencies of the thickness modes. In order to improve the accuracy of the dispersion relations and eliminating the need of correction factors, the new series expansion of [7] will be used for deriving the 2-D equations in the present paper.

For a plate referred to the rectangular coordinates $x_i$ as shown in Fig. 1, the new series expansions of the displacement and electric potential are [7]:

$$u_i = -u^{(0)}_{2,i}x_2 + \sum_{n=0}^{\infty} u_i^{(n)} \cos\frac{n\pi}{2}(1-\psi), i = 1,2,3,$$
$$\phi = \bar{V}_0(t) + \bar{V}_1(t)\psi\frac{b}{b_q} + \sum_{n=0}^{\infty}\phi^{(n)}\sin\frac{n\pi}{2}(1-\psi), \tag{4}$$

where $\psi = x_2/b$, $u_i^{(n)}$ and $\phi^{(n)}$ are functions of $x_1$, $x_3$, and time $t$, $2b$ and $2b_q$ are the thicknesses of the composite plate and crystal, respectively, as shown in Fig. 2, and $\bar{V}_0$, $\bar{V}_1$ are determined by the specified electric potential at the electroded surfaces.

Insertion of (4) into (3) leads to the series expansions of strain and electric field

$$S_{ij} = S^d_{ij}\psi + \sum_{n=0}^{\infty}\left[S^{(n)}_{ij}\cos\frac{n\pi}{2}(1-\psi) + \bar{S}^{(n)}_{ij}\sin\frac{n\pi}{2}(1-\psi)\right],$$
$$E_i = \sum_{n=0}^{\infty}\left[E_i^{(n)}\sin\frac{n\pi}{2}(1-\psi) + \bar{E}_i^{(n)}\cos\frac{n\pi}{2}(1-\psi)\right], \tag{5}$$

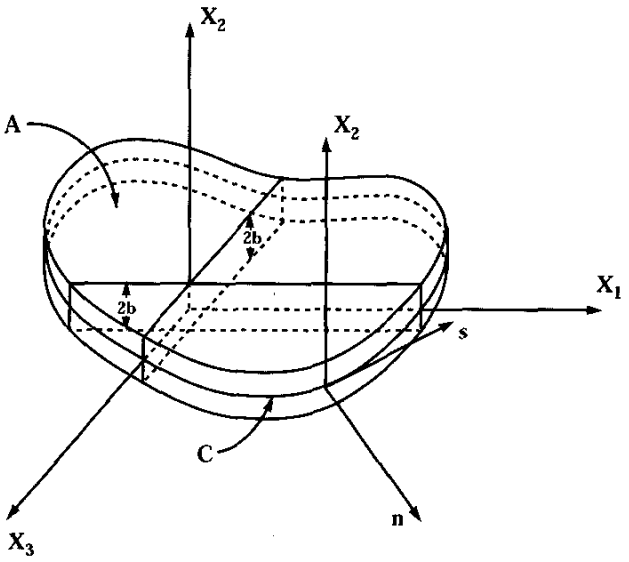


Fig. 1. A plate of uniform thickness referred to the $x_i$ coordinate system.

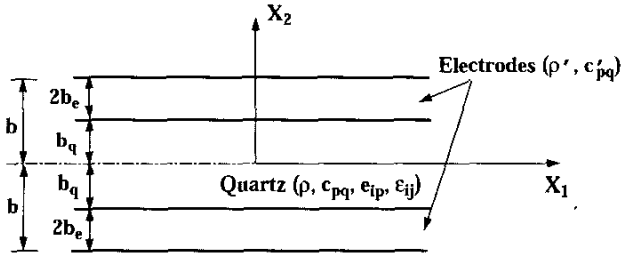


Fig. 2. A composite plate of quartz crystal and two identical electrodes.

where

$$S^d_{ij} = -bu^{(0)}_{2,ij},$$
$$S^{(n)}_{ij} = \frac{1}{2}\left[u^{(n)}_{i,j} + u^{(n)}_{j,i} - \delta_{n0}\left(\delta_{2j}u^{(0)}_{2,i} + \delta_{2i}u^{(0)}_{2,j}\right)\right],$$
$$\bar{S}^{(n)}_{ij} = \frac{n\pi}{4b}\left(\delta_{2i}u^{(n)}_j + \delta_{2j}u^{(n)}_i\right),$$
$$E^{(n)}_i = -\phi^{(n)}_{,i},$$
$$\bar{E}^{(n)}_i = -\delta_{2i}\delta_{n0}\frac{\bar{V}_1}{b_q} + \delta_{2i}\frac{n\pi}{2b}\phi^{(n)}, \tag{6}$$

and $\delta_{ij}$ is the Kronecker delta.

By substituting (4) into $(1)_1$, setting $dV = bd\psi dA$ with $dA = dx_1dx_3$, and integrating with respect to $\psi$ from $-1$

to 1, we obtain:

$$\begin{aligned}\int_{t0}^{t} dt \int_A \Bigg\{ \sum_{n=0}^{\infty} \Bigg[ & T_{aj,a}^{(n)} - \frac{n\pi}{2b}\bar{T}_{2j}^{(n)} + \frac{1}{b}F_j^{(n)} \\ & - \sum_{m=0}^{\infty} \frac{1}{2}\left(\rho^{(m+n)} + \rho^{(m-n)}\right)\ddot{u}_j^{(m)} + b\hat{\rho}^{(n)}\ddot{u}_{2,j}^{(0)} \Bigg] \delta u_j^{(n)} \\ & - \Bigg( T_{aj,a}^{d} - \frac{1}{b}T_{2j}^{(0)} + \frac{1}{b}F_j^{(1)} \\ & - \sum_{m=0}^{\infty} \hat{\rho}^{(m)}\ddot{u}_j^{(m)} + b\rho^{d}\ddot{u}_{2,j}^{(0)} \Bigg) b\delta u_{2,j}^{(0)} \\ & + \sum_{n=0}^{\infty} \left( \bar{D}_{a,a}^{(n)} + \frac{n\pi}{2b}D_2^{(n)} \right) \delta\phi^{(n)} \Bigg\} dA = 0,\end{aligned} \tag{7}$$

where $a = 1, 3$, and

$$\begin{aligned} T_{ij}^{d} &= \int_{-1}^{1} T_{ij}\psi d\psi, \\ T_{ij}^{(n)} &= \int_{-1}^{1} T_{ij}\cos\frac{n\pi}{2}(1-\psi)d\psi, \\ \bar{T}_{ij}^{(n)} &= \int_{-1}^{1} T_{ij}\sin\frac{n\pi}{2}(1-\psi)d\psi, \\ D_i^{(n)} &= \int_{-1}^{1} D_i\cos\frac{n\pi}{2}(1-\psi)d\psi, \\ \bar{D}_i^{(n)} &= \int_{-1}^{1} D_i\sin\frac{n\pi}{2}(1-\psi)d\psi, \\ F_j^{(n)} &= T_{2j}(b) - (-1)^n T_{2j}(-b); \end{aligned} \tag{8}$$

$$\begin{aligned} \rho^{(n)} &= \int_{-1}^{1} \rho\cos\frac{n\pi}{2}(1-\psi)d\psi, \\ \hat{\rho}^{(n)} &= \int_{-1}^{1} \rho\psi\cos\frac{n\pi}{2}(1-\psi)d\psi, \\ \rho^{d} &= \int_{-1}^{1} \rho\psi^2 d\psi. \end{aligned} \tag{9}$$

Note that, in (7), the thickness-graded mass density of the plate has been assumed as a function of the thickness coordinate, and the effective mass densities $\rho^{(n)}$, $\hat{\rho}^{(n)}$, and $\rho^{d}$ are defined in (9).

By using Fourier series expansion, the linear function $\psi$ can be expressed by, for $-1 < \psi < 1$,

$$\psi = \sum_{n=0}^{\infty} c_n \cos\frac{n\pi}{2}(1-\psi), \tag{10}$$

where

$$c_n = \int_{-1}^{1} \psi\cos\frac{n\pi}{2}(1-\psi)d\psi = \begin{cases} \dfrac{8}{n^2\pi^2}, & n = \text{odd} \\ 0, & n = \text{even} \end{cases} \tag{11}$$

By substituting (10) into $(8)_1$ and $(9)_{2,3}$, we obtain

$$\begin{aligned} T_{ij}^{d} &= \sum_{n=0}^{\infty} c_n T_{ij}^{(n)}. \\ \hat{\rho}^{(m)} &= \sum_{n=0}^{\infty} \frac{1}{2}c_n\left(\rho^{(m+n)} + \rho^{(m-n)}\right), \\ \rho^{d} &= \sum_{n=0}^{\infty} c_n\hat{\rho}^{(n)}. \end{aligned} \tag{12}$$

By the integration by parts, we have

$$\int_{-1}^{1} T_{2j,2}\psi d\psi = -\frac{1}{b}T_{2j}^{(0)} + \frac{1}{b}F_j^{(1)}. \tag{13}$$

By substituting (10) into the left-hand side of (13) and using the integration by parts again, we obtain:

$$-\frac{1}{b}T_{2j}^{(0)} + \frac{1}{b}F_j^{(1)} = \sum_{n=0}^{\infty} c_n\left(\frac{1}{b}F_j^{(n)} - \frac{n\pi}{2b}\bar{T}_{2j}^{(n)}\right). \tag{14}$$

Further substitution of (12) and (14) into the terms enclosed by the second bracket of (7) leads to:

$$\begin{aligned}\int_{t0}^{t} dt \int_A \Bigg\{ \sum_{n=0}^{\infty} \Bigg[ & T_{aj,a}^{(n)} - \frac{n\pi}{2b}\bar{T}_{2j}^{(n)} + \frac{1}{b}F_j^{(n)} + b\hat{\rho}^{(n)}\ddot{u}_{2,j}^{(0)} \\ & - \sum_{m=0}^{\infty} \frac{1}{2}\left(\rho^{(m+n)} + \rho^{(m-n)}\right)\ddot{u}_j^{(m)} \Bigg] \delta\left(u_j^{(n)} - c_n b u_{2,j}^{(0)}\right) \\ & + \sum_{n=0}^{\infty} \left( \bar{D}_{a,a}^{(n)} + \frac{n\pi}{2b}D_2^{(n)} \right) \delta\phi^{(n)} \Bigg\} dA = 0.\end{aligned} \tag{15}$$

Thus, for arbitrary variations $\delta\left(u_j^{(n)} - c_n b u_{2,j}^{(0)}\right)$ and $\delta\phi^{(n)}$, we have, in $A$:

$$\begin{aligned} & T_{aj,a}^{(n)} - \frac{n\pi}{2b}\bar{T}_{2j}^{(n)} + \frac{1}{b}F_j^{(n)} \\ & = \sum_{m=0}^{\infty} \frac{1}{2}\left(\rho^{(m+n)} + \rho^{(m-n)}\right)\ddot{u}_j^{(m)} - b\hat{\rho}^{(n)}\ddot{u}_{2,j}^{(0)}, \\ & \bar{D}_{a,a}^{(n)} + \frac{n\pi}{2b}D_2^{(n)} = 0, \end{aligned} \tag{16}$$

where $n = 0, 1, 2, \cdots$, and $\bar{D}_a^{(0)} = 0$ by definition.

In a similar manner, substituting (4) into $(1)_2$, noting that $S = A^+ + A^- + A'$, where $A^+$, $A^-$ are the upper and lower surfaces, $A'$ the lateral surface, and $dA' = bd\psi ds$ with $s$ being the coordinate measured along the curve of the edge $C$ as shown in Fig. 1, we obtain:

$$\begin{aligned}\int_{t_0}^{t} dt \Bigg\{ & \int_{A^+ + A^-} \left[ \left(t_j - n_i T_{ij}\right)\delta u_j - \left(\sigma + n_i D_i\right)\delta\phi \right] dA \\ & + b\oint_C \Bigg[ \sum_{n=0}^{\infty} \left(t_j^{(n)} - n_i T_{ij}^{(n)}\right)\delta u_j^{(n)} - \left(t_j^{d} - n_i T_{ij}^{d}\right) b\delta u_{2,j}^{(0)} \\ & - \sum_{n=0}^{\infty} \left(\bar{\sigma}^{(n)} + n_i\bar{D}_i^{(n)}\right)\delta\phi^{(n)} \Bigg] ds \Bigg\} = 0,\end{aligned} \tag{17}$$

where

$$t_j^d = \int_{-1}^{1} t_j \psi d\psi,$$
$$t_j^{(n)} = \int_{-1}^{1} t_j \cos\frac{n\pi}{2}(1-\psi)d\psi, \tag{18}$$
$$\bar{\sigma}^{(n)} = \int_{-1}^{1} \sigma \sin\frac{n\pi}{2}(1-\psi)d\psi.$$

Again, by substituting (10) into $(18)_1$ and using $(18)_2$, we obtain:

$$t_j^d = \sum_{n=0}^{\infty} c_n t_j^{(n)}. \tag{19}$$

The surface integral in (17) vanishes by specifying the face tractions, $t_j = n_i T_{ij}$, through the definition of $F_j^{(n)}$ in $(8)_6$, and the electric potentials at the electrodes through $\bar{V}_0, \bar{V}_1$ in $(4)_2$. By using (19) and $(12)_1$, the remaining part of (17) becomes:

$$\int_{t_0}^{t} dt \oint_C \left[ \sum_{n=0}^{\infty} \left( t_j^{(n)} - n_i T_{ij}^{(n)} \right) \delta \left( u_j^{(n)} - c_n b u_{2,j}^{(0)} \right) - \sum_{n=0}^{\infty} \left( \bar{\sigma}^{(n)} + n_i \bar{D}_i^{(n)} \right) \delta\phi^{(n)} \right] ds = 0. \tag{20}$$

Hence, we have the edge conditions on $C$:

$$t_j^{(n)} = n_i T_{ij}^{(n)} \text{ or } \quad u_j^{(n)} - c_n b u_{2,j}^{(0)} = \hat{u}_j^{(n)} - c_n b \hat{u}_{2,j}^{(0)},$$
$$\bar{\sigma}^{(n)} = -n_i \bar{D}_i^{(n)} \text{ or } \quad \phi^{(n)} = \hat{\phi}^{(n)}, \tag{21}$$

where $n = 0, 1, 2, \cdots$, and $\hat{u}_j^{(n)}$, $\hat{\phi}^{(n)}$ are prescribed values of the $n$th-order displacements and electric potentials on $C$.

The 2-D constitutive relations for plates with thickness-graded material properties are obtained by inserting (5) into (2) and then into $(8)_{2-5}$,

$$\begin{aligned} T_{ij}^{(n)} &= \hat{c}_{ijkl}^{(n)} S_{kl}^d + \frac{1}{2}\sum_{m=0}^{\infty} \Big[ \left( c_{ijkl}^{(m+n)} + c_{ijkl}^{(m-n)} \right) S_{kl}^{(m)} \\ &+ \left( \bar{c}_{ijkl}^{(m+n)} + \bar{c}_{ijkl}^{(m-n)} \right) \bar{S}_{kl}^{(m)} \\ &- \left( \bar{e}_{kij}^{(m+n)} + \bar{e}_{kij}^{(m-n)} \right) E_k^{(m)} \\ &- \left( e_{kij}^{(m+n)} + e_{kij}^{(m-n)} \right) \bar{E}_k^{(m)} \Big], \end{aligned}$$

$$\begin{aligned} \bar{T}_{ij}^{(n)} &= \tilde{c}_{ijkl}^{(n)} S_{kl}^d + \frac{1}{2}\sum_{m=0}^{\infty} \Big[ \left( \bar{c}_{ijkl}^{(m+n)} - \bar{c}_{ijkl}^{(m-n)} \right) S_{kl}^{(m)} \\ &+ \left( -c_{ijkl}^{(m+n)} + c_{ijkl}^{(m-n)} \right) \bar{S}_{kl}^{(m)} \\ &- \left( -e_{kij}^{(m+n)} + e_{kij}^{(m-n)} \right) E_k^{(m)} \\ &- \left( \bar{e}_{kij}^{(m+n)} - \bar{e}_{kij}^{(m-n)} \right) \bar{E}_k^{(m)} \Big], \end{aligned}$$

$$\begin{aligned} D_i^{(n)} &= \hat{e}_{ijk}^{(n)} S_{jk}^d + \frac{1}{2}\sum_{m=0}^{\infty} \Big[ \left( e_{ijk}^{(m+n)} + e_{ijk}^{(m-n)} \right) S_{jk}^{(m)} \\ &+ \left( \bar{e}_{ijk}^{(m+n)} + \bar{e}_{ijk}^{(m-n)} \right) \bar{S}_{jk}^{(m)} \\ &+ \left( \bar{\epsilon}_{ij}^{(m+n)} + \bar{\epsilon}_{ij}^{(m-n)} \right) E_j^{(m)} \\ &+ \left( \epsilon_{ij}^{(m+n)} + \epsilon_{ij}^{(m-n)} \right) \bar{E}_j^{(m)} \Big], \end{aligned} \tag{22}$$

$$\begin{aligned} \bar{D}_i^{(n)} &= \tilde{e}_{ijk}^{(n)} S_{jk}^d + \frac{1}{2}\sum_{m=0}^{\infty} \Big[ \left( \bar{e}_{ijk}^{(m+n)} - \bar{e}_{ijk}^{(m-n)} \right) S_{jk}^{(m)} \\ &+ \left( -e_{ijk}^{(m+n)} + e_{ijk}^{(m-n)} \right) \bar{S}_{jk}^{(m)} \\ &+ \left( -\epsilon_{ij}^{(m+n)} + \epsilon_{ij}^{(m-n)} \right) E_j^{(m)} \\ &+ \left( \bar{\epsilon}_{ij}^{(m+n)} - \bar{\epsilon}_{ij}^{(m-n)} \right) \bar{E}_j^{(m)} \Big], \end{aligned}$$

where

$$\begin{aligned} \mathcal{M}^{(n)} &= \int_{-1}^{1} \mathcal{M}(\psi) \cos\frac{n\pi}{2}(1-\psi)d\psi, \\ \bar{\mathcal{M}}^{(n)} &= \int_{-1}^{1} \mathcal{M}(\psi) \sin\frac{n\pi}{2}(1-\psi)d\psi, \\ \hat{\mathcal{M}}^{(n)} &= \int_{-1}^{1} \mathcal{M}(\psi)\psi \cos\frac{n\pi}{2}(1-\psi)d\psi, \\ \tilde{\mathcal{M}}^{(n)} &= \int_{-1}^{1} \mathcal{M}(\psi)\psi \sin\frac{n\pi}{2}(1-\psi)d\psi, \end{aligned} \tag{23}$$

and $\mathcal{M}(\psi)$ stands for any thickness-graded material property, $c_{ijkl}$, $e_{ijk}$, or $\epsilon_{ij}$. For homogeneous plates with uniform material properties, (22) reduces to the constitutive equations obtained in [7].

## III. First-Order Equations

To extract a finite set of first-order approximate equations from the infinite system of 2-D equations in the preceding section, we let:

$$\begin{aligned} &u_1^{(n)} = u_3^{(n)} = 0, \quad n > 1, \\ &u_2^{(n)} = 0, \phi^{(n)} = 0, \quad n > 2, \\ &T_{22}^{(1)} = 0, \ddot{u}_2^{(2)} = 0, \end{aligned} \tag{24}$$

and disregard $T_{ij}^{(n)}$, $\bar{T}_{ij}^{(n)}$, $D_i^{(n+1)}$, $\bar{D}_i^{(n+1)}$, and $S_{ij}^{(n)}$ for $n > 1$.

Accordingly, the field equations in (16) reduce to:

$$\begin{aligned}
&T^{(0)}_{aj,a} + \frac{1}{b}F^{(0)}_j = \rho^{(0)}\ddot{u}^{(0)}_j + \rho^{(1)}\ddot{u}^{(1)}_j - \hat{\rho}^{(0)}b\ddot{u}^{(0)}_{2,j},\\
&T^{(1)}_{aj,a} - \frac{\pi}{2b}\bar{T}^{(1)}_{2j} + \frac{1}{b}F^{(1)}_j = \rho^{(1)}\ddot{u}^{(0)}_j\\
&\qquad + \frac{1}{2}\left(\rho^{(0)} + \rho^{(2)}\right)\ddot{u}^{(1)}_j - \hat{\rho}^{(1)}b\ddot{u}^{(0)}_{2,j},\\
&\bar{D}^{(1)}_{a,a} + \frac{\pi}{2b}D^{(1)}_2 = 0,\\
&\bar{D}^{(2)}_{a,a} + \frac{\pi}{b}D^{(2)}_2 = 0.
\end{aligned} \tag{25}$$

From the constitutive relations in (22), in terms of the contracted notation, we have

$$\begin{aligned}
T^{(1)}_2 &= \hat{c}^{(1)}_{2q}S^d_q + c^{(1)}_{2q}S^{(0)}_q + \frac{1}{2}\left(c^{(0)}_{2q} + c^{(2)}_{2q}\right)S^{(1)}_q\\
&+\frac{1}{2}\bar{c}^{(2)}_{2q}\bar{S}^{(1)}_q + \frac{1}{2}\left(\bar{c}^{(1)}_{2q} + \bar{c}^{(3)}_{2q}\right)\bar{S}^{(2)}_q - \frac{1}{2}\bar{e}^{(2)}_{k2}E^{(1)}_k\\
&\quad -\frac{1}{2}\left(\bar{e}^{(1)}_{k2} + \bar{e}^{(3)}_{k2}\right)E^{(2)}_k - e^{(1)}_{k2}\bar{E}^{(0)}_k\\
&-\frac{1}{2}\left(e^{(0)}_{k2} + e^{(2)}_{k2}\right)\bar{E}^{(1)}_k - \frac{1}{2}\left(e^{(1)}_{k2} + e^{(3)}_{k2}\right)\bar{E}^{(2)}_k.
\end{aligned} \tag{26}$$

By imposing $T^{(1)}_2 = 0$ and solving for $\bar{S}^{(2)}_2 = \dfrac{\pi}{b}u^{(2)}_2$, we obtain:

$$\begin{aligned}
\bar{S}^{(2)}_2 &= -\frac{2}{\bar{c}^{(1)}_{22} + \bar{c}^{(3)}_{22}}\left[\hat{c}^{(1)}_{2q}S^d_q + c^{(1)}_{2q}S^{(0)}_q\right.\\
&+\frac{1}{2}\left(c^{(0)}_{2q} + c^{(2)}_{2q}\right)S^{(1)}_q + \frac{1}{2}\bar{c}^{(2)}_{2q}\bar{S}^{(1)}_q - \frac{1}{2}\bar{e}^{(2)}_{k2}E^{(1)}_k\\
&\quad -\frac{1}{2}\left(\bar{e}^{(1)}_{k2} + \bar{e}^{(3)}_{k2}\right)E^{(2)}_k - e^{(1)}_{k2}\bar{E}^{(0)}_k\\
&\left.-\frac{1}{2}\left(e^{(0)}_{k2} + e^{(2)}_{k2}\right)\bar{E}^{(1)}_k - \frac{1}{2}\left(e^{(1)}_{k2} + e^{(3)}_{k2}\right)\bar{E}^{(2)}_k\right].
\end{aligned} \tag{27}$$

Substitution of (27) into the remaining relations of (22) eliminates $\bar{S}^{(2)}_2$ from the constitutive relations and thus $u^{(2)}_2$ does not appear in the first-order equations. The resulting constitutive relations, in the contracted notations, are:

$$\begin{aligned}
T^{(0)}_p &= c^{(0d)}_{pq}S^d_q + c^{(00)}_{pq}S^{(0)}_q + c^{(01)}_{pq}S^{(1)}_q + c^{(0\bar{1})}_{pq}\bar{S}^{(1)}_q\\
&\quad - \bar{e}^{(10)}_{kp}E^{(1)}_k - \bar{e}^{(20)}_{kp}E^{(2)}_k - \bar{e}^{(\bar{0}0)}_{kp}\bar{E}^{(0)}_k\\
&\quad - \bar{e}^{(\bar{1}0)}_{kp}\bar{E}^{(1)}_k - \bar{e}^{(\bar{2}0)}_{kp}\bar{E}^{(2)}_k,\\
T^{(1)}_p &= c^{(1d)}_{pq}S^d_q + c^{(10)}_{pq}S^{(0)}_q + c^{(11)}_{pq}S^{(1)}_q + c^{(1\bar{1})}_{pq}\bar{S}^{(1)}_q\\
&\quad - \bar{e}^{(11)}_{kp}E^{(1)}_k - \bar{e}^{(21)}_{kp}E^{(2)}_k - \bar{e}^{(\bar{0}1)}_{kp}\bar{E}^{(0)}_k\\
&\quad - \bar{e}^{(\bar{1}1)}_{kp}\bar{E}^{(1)}_k - \bar{e}^{(\bar{2}1)}_{kp}\bar{E}^{(2)}_k,
\end{aligned}$$

$$\begin{aligned}
\bar{T}^{(1)}_p &= c^{(\bar{1}d)}_{pq}S^d_q + c^{(\bar{1}0)}_{pq}S^{(0)}_q + c^{(\bar{1}1)}_{pq}S^{(1)}_q + c^{(\bar{1}\bar{1})}_{pq}\bar{S}^{(1)}_q\\
&\quad - \bar{e}^{(1\bar{1})}_{kp}E^{(1)}_k - \bar{e}^{(2\bar{1})}_{kp}E^{(2)}_k - \bar{e}^{(\bar{0}\bar{1})}_{kp}\bar{E}^{(0)}_k\\
&\quad - \bar{e}^{(\bar{1}\bar{1})}_{kp}\bar{E}^{(1)}_k - \bar{e}^{(\bar{2}\bar{1})}_{kp}\bar{E}^{(2)}_k,\\
D^{(1)}_i &= e^{(1d)}_{iq}S^d_q + e^{(10)}_{iq}S^{(0)}_q + e^{(11)}_{iq}S^{(1)}_q + e^{(1\bar{1})}_{iq}\bar{S}^{(1)}_q\\
&\quad + \epsilon^{(11)}_{ik}E^{(1)}_k + \epsilon^{(12)}_{ik}E^{(2)}_k + \epsilon^{(1\bar{0})}_{ik}\bar{E}^{(0)}_k\\
&\quad + \epsilon^{(1\bar{1})}_{ik}\bar{E}^{(1)}_k + \epsilon^{(1\bar{2})}_{ik}\bar{E}^{(2)}_k,\\
D^{(2)}_i &= e^{(2d)}_{iq}S^d_q + e^{(20)}_{iq}S^{(0)}_q + e^{(21)}_{iq}S^{(1)}_q + e^{(2\bar{1})}_{iq}\bar{S}^{(1)}_q\\
&\quad + \epsilon^{(21)}_{ik}E^{(1)}_k + \epsilon^{(22)}_{ik}E^{(2)}_k + \epsilon^{(2\bar{0})}_{ik}\bar{E}^{(0)}_k\\
&\quad + \epsilon^{(2\bar{1})}_{ik}\bar{E}^{(1)}_k + \epsilon^{(2\bar{2})}_{ik}\bar{E}^{(2)}_k,\\
\bar{D}^{(1)}_i &= e^{(\bar{1}d)}_{iq}S^d_q + e^{(\bar{1}0)}_{iq}S^{(0)}_q + e^{(\bar{1}1)}_{iq}S^{(1)}_q + e^{(\bar{1}\bar{1})}_{iq}\bar{S}^{(1)}_q\\
&\quad + \epsilon^{(\bar{1}1)}_{ik}E^{(1)}_k + \epsilon^{(\bar{1}2)}_{ik}E^{(2)}_k + \epsilon^{(\bar{1}\bar{0})}_{ik}\bar{E}^{(0)}_k\\
&\quad + \epsilon^{(\bar{1}\bar{1})}_{ik}\bar{E}^{(1)}_k + \epsilon^{(\bar{1}\bar{2})}_{ik}\bar{E}^{(2)}_k,\\
\bar{D}^{(2)}_i &= e^{(\bar{2}d)}_{iq}S^d_q + e^{(\bar{2}0)}_{iq}S^{(0)}_q + e^{(\bar{2}1)}_{iq}S^{(1)}_q + e^{(\bar{2}\bar{1})}_{iq}\bar{S}^{(1)}_q\\
&\quad + \epsilon^{(\bar{2}1)}_{ik}E^{(1)}_k + \epsilon^{(\bar{2}2)}_{ik}E^{(2)}_k + \epsilon^{(\bar{2}\bar{0})}_{ik}\bar{E}^{(0)}_k\\
&\quad + \epsilon^{(\bar{2}\bar{1})}_{ik}\bar{E}^{(1)}_k + \epsilon^{(\bar{2}\bar{2})}_{ik}\bar{E}^{(2)}_k,
\end{aligned} \tag{28}$$

where

$$\begin{aligned}
c^{(nd)}_{pq} &= \hat{c}^{(n)}_{pq} - \frac{\bar{c}^{(2+n)}_{p2} + \bar{c}^{(2-n)}_{p2}}{\bar{c}^{(1)}_{22} + \bar{c}^{(3)}_{22}}\hat{c}^{(1)}_{2q},\\
c^{(\bar{n}d)}_{pq} &= \tilde{c}^{(n)}_{pq} - \frac{-c^{(2+n)}_{p2} + c^{(2-n)}_{p2}}{\bar{c}^{(1)}_{22} + \bar{c}^{(3)}_{22}}\hat{c}^{(1)}_{2q},\\
e^{(nd)}_{ip} &= \hat{e}^{(n)}_{ip} - \frac{\bar{e}^{(2+n)}_{i2} + \bar{e}^{(2-n)}_{i2}}{\bar{c}^{(1)}_{22} + \bar{c}^{(3)}_{22}}\hat{c}^{(1)}_{2p},\\
e^{(\bar{n}d)}_{ip} &= \tilde{e}^{(n)}_{ip} - \frac{-e^{(2+n)}_{i2} + e^{(2-n)}_{i2}}{\bar{c}^{(1)}_{22} + \bar{c}^{(3)}_{22}}\hat{c}^{(1)}_{2p};
\end{aligned} \tag{29}$$

$$\begin{aligned}
c^{(nm)}_{pq} &= \frac{1}{2}\left(c^{(m+n)}_{pq} + c^{(m-n)}_{pq}\right)\\
&\quad - \frac{1}{2}\left(\bar{c}^{(2+n)}_{p2} + \bar{c}^{(2-n)}_{p2}\right)\frac{c^{(m+1)}_{2q} + c^{(m-1)}_{2q}}{\bar{c}^{(1)}_{22} + \bar{c}^{(3)}_{22}},\\
c^{(n\bar{m})}_{pq} &= \frac{1}{2}\left(\bar{c}^{(m+n)}_{pq} + \bar{c}^{(m-n)}_{pq}\right)\\
&\quad - \frac{1}{2}\left(\bar{c}^{(2+n)}_{p2} + \bar{c}^{(2-n)}_{p2}\right)\frac{\bar{c}^{(m+1)}_{2q} + \bar{c}^{(m-1)}_{2q}}{\bar{c}^{(1)}_{22} + \bar{c}^{(3)}_{22}},\\
c^{(\bar{n}m)}_{pq} &= \frac{1}{2}\left(\bar{c}^{(m+n)}_{pq} - \bar{c}^{(m-n)}_{pq}\right)\\
&\quad - \frac{1}{2}\left(-c^{(2+n)}_{p2} + c^{(2-n)}_{p2}\right)\frac{c^{(m+1)}_{2q} + c^{(m-1)}_{2q}}{\bar{c}^{(1)}_{22} + \bar{c}^{(3)}_{22}},\\
c^{(\bar{n}\bar{m})}_{pq} &= \frac{1}{2}\left(-c^{(m+n)}_{pq} + c^{(m-n)}_{pq}\right)\\
&\quad - \frac{1}{2}\left(-c^{(2+n)}_{p2} + c^{(2-n)}_{p2}\right)\frac{\bar{c}^{(m+1)}_{2q} + \bar{c}^{(m-1)}_{2q}}{\bar{c}^{(1)}_{22} + \bar{c}^{(3)}_{22}};
\end{aligned} \tag{30}$$

$$
\begin{aligned}
e_{ip}^{(nm)} &= \frac{1}{2}\left(e_{ip}^{(m+n)} + e_{ip}^{(m-n)}\right) \\
&\quad - \frac{1}{2}\left(\bar{e}_{i2}^{(2+n)} + \bar{e}_{i2}^{(2-n)}\right)\frac{c_{2p}^{(m+1)} + c_{2p}^{(m-1)}}{\bar{c}_{22}^{(1)} + \bar{c}_{22}^{(3)}}, \\
e_{ip}^{(n\bar{m})} &= \frac{1}{2}\left(\bar{e}_{ip}^{(m+n)} + \bar{e}_{ip}^{(m-n)}\right) \\
&\quad - \frac{1}{2}\left(\bar{e}_{i2}^{(2+n)} + \bar{e}_{i2}^{(2-n)}\right)\frac{\bar{c}_{2p}^{(m+1)} + \bar{c}_{2p}^{(m-1)}}{\bar{c}_{22}^{(1)} + \bar{c}_{22}^{(3)}}, \\
e_{ip}^{(\bar{n}m)} &= \frac{1}{2}\left(\bar{e}_{ip}^{(m+n)} - \bar{e}_{ip}^{(m-n)}\right) \\
&\quad - \frac{1}{2}\left(-e_{i2}^{(2+n)} + e_{i2}^{(2-n)}\right)\frac{c_{2p}^{(m+1)} + c_{2p}^{(m-1)}}{\bar{c}_{22}^{(1)} + \bar{c}_{22}^{(3)}}, \\
e_{ip}^{(\bar{n}\bar{m})} &= \frac{1}{2}\left(-e_{ip}^{(m+n)} + e_{ip}^{(m-n)}\right) \\
&\quad - \frac{1}{2}\left(-e_{i2}^{(2+n)} + e_{i2}^{(2-n)}\right)\frac{\bar{c}_{2p}^{(m+1)} + \bar{c}_{2p}^{(m-1)}}{\bar{c}_{22}^{(1)} + \bar{c}_{22}^{(3)}}; \\
\bar{e}_{ip}^{(mn)} &= \frac{1}{2}\left(\bar{e}_{ip}^{(m+n)} + \bar{e}_{ip}^{(m-n)}\right) \\
&\quad - \frac{1}{2}\left(\bar{c}_{p2}^{(2+n)} + \bar{c}_{p2}^{(2-n)}\right)\frac{\bar{e}_{i2}^{(m+1)} + \bar{e}_{i2}^{(m-1)}}{\bar{c}_{22}^{(1)} + \bar{c}_{22}^{(3)}}, \\
\bar{e}_{ip}^{(\bar{m}n)} &= \frac{1}{2}\left(e_{ip}^{(m+n)} + e_{ip}^{(m-n)}\right) \\
&\quad - \frac{1}{2}\left(\bar{c}_{p2}^{(2+n)} + \bar{c}_{p2}^{(2-n)}\right)\frac{e_{i2}^{(m+1)} + e_{i2}^{(m-1)}}{\bar{c}_{22}^{(1)} + \bar{c}_{22}^{(3)}}, \\
\bar{e}_{ip}^{(m\bar{n})} &= \frac{1}{2}\left(-e_{ip}^{(m+n)} + e_{ip}^{(m-n)}\right) \\
&\quad - \frac{1}{2}\left(-c_{p2}^{(2+n)} + c_{p2}^{(2-n)}\right)\frac{\bar{e}_{i2}^{(m+1)} + \bar{e}_{i2}^{(m-1)}}{\bar{c}_{22}^{(1)} + \bar{c}_{22}^{(3)}}, \\
\bar{e}_{ip}^{(\bar{m}\bar{n})} &= \frac{1}{2}\left(\bar{e}_{ip}^{(m+n)} - \bar{e}_{ip}^{(m-n)}\right) \\
&\quad - \frac{1}{2}\left(-c_{p2}^{(2+n)} + c_{p2}^{(2-n)}\right)\frac{e_{i2}^{(m+1)} + e_{i2}^{(m-1)}}{\bar{c}_{22}^{(1)} + \bar{c}_{22}^{(3)}}; \\
\epsilon_{ij}^{(nm)} &= \frac{1}{2}\left(\bar{\epsilon}_{ij}^{(m+n)} + \bar{\epsilon}_{ij}^{(m-n)}\right) \\
&\quad + \frac{1}{2}\left(\bar{e}_{i2}^{(2+n)} + \bar{e}_{i2}^{(2-n)}\right)\frac{\bar{e}_{j2}^{(m+1)} + \bar{e}_{j2}^{(m-1)}}{\bar{c}_{22}^{(1)} + \bar{c}_{22}^{(3)}}, \\
\epsilon_{ij}^{(n\bar{m})} &= \frac{1}{2}\left(\epsilon_{ij}^{(m+n)} + \epsilon_{ij}^{(m-n)}\right) \\
&\quad + \frac{1}{2}\left(\bar{e}_{i2}^{(2+n)} + \bar{e}_{i2}^{(2-n)}\right)\frac{e_{j2}^{(m+1)} + e_{j2}^{(m-1)}}{\bar{c}_{22}^{(1)} + \bar{c}_{22}^{(3)}}, \\
\epsilon_{ij}^{(\bar{n}m)} &= \frac{1}{2}\left(-\epsilon_{ij}^{(m+n)} + \epsilon_{ij}^{(m-n)}\right) \\
&\quad + \frac{1}{2}\left(-e_{i2}^{(2+n)} + e_{i2}^{(2-n)}\right)\frac{\bar{e}_{j2}^{(m+1)} + \bar{e}_{j2}^{(m-1)}}{\bar{c}_{22}^{(1)} + \bar{c}_{22}^{(3)}}, \\
\epsilon_{ij}^{(\bar{n}\bar{m})} &= \frac{1}{2}\left(\bar{\epsilon}_{ij}^{(m+n)} - \bar{\epsilon}_{ij}^{(m-n)}\right) \\
&\quad + \frac{1}{2}\left(-e_{i2}^{(2+n)} + e_{i2}^{(2-n)}\right)\frac{e_{j2}^{(m+1)} + e_{j2}^{(m-1)}}{\bar{c}_{22}^{(1)} + \bar{c}_{22}^{(3)}}.
\end{aligned}
\tag{31}
\tag{32}
\tag{33}
$$

The strain-displacement relations and electric field-potential relations for the first-order equations are obtained from (6),

$$
\begin{aligned}
&S_1^d = -bu_{2,11}^{(0)}, S_5^d = -2bu_{2,13}^{(0)}, S_3^d = -bu_{2,33}^{(0)}, \\
&S_1^{(0)} = u_{1,1}^{(0)}, S_5^{(0)} = u_{3,1}^{(0)} + u_{1,3}^{(0)}, S_3^{(0)} = u_{3,3}^{(0)}, \\
&S_1^{(1)} = u_{1,1}^{(1)}, S_5^{(1)} = u_{3,1}^{(1)} + u_{1,3}^{(1)}, S_3^{(1)} = u_{3,3}^{(1)}, \\
&S_6^{(1)} = u_{2,1}^{(1)}, S_4^{(1)} = u_{2,3}^{(1)}, \bar{S}_6^{(1)} = \frac{\pi}{2b}u_1^{(1)}, \\
&\bar{S}_2^{(1)} = \frac{\pi}{2b}u_2^{(1)}, \bar{S}_4^{(1)} = \frac{\pi}{2b}u_3^{(1)}, E_1^{(1)} = -\phi_{,1}^{(1)}, \\
&\bar{E}_2^{(0)} = -\bar{V}_1/b_q, E_3^{(1)} = -\phi_{,3}^{(1)}, E_1^{(2)} = -\phi_{,1}^{(2)}, \\
&\bar{E}_2^{(1)} = \frac{\pi}{2b}\phi^{(1)}, E_3^{(2)} = -\phi_{,3}^{(2)}, \bar{E}_2^{(2)} = \frac{\pi}{b}\phi^{(2)}.
\end{aligned}
\tag{34}
$$

From (21), the edge conditions for the first-order equations are:

$$
\begin{aligned}
&t_j^{(0)} = n_i T_{ij}^{(0)} \text{ or } \quad u_j^{(0)} = \hat{u}_j^{(0)}, \\
&t_j^{(1)} = n_i T_{ij}^{(1)} \text{ or } \quad u_j^{(1)} - \frac{8}{\pi^2}bu_{2,j}^{(0)} = \hat{u}_j^{(1)} - \frac{8}{\pi^2}b\hat{u}_{2,j}^{(0)}, \\
&\bar{\sigma}^{(1)} = -n_i\bar{D}_i^{(1)} \text{ or } \quad \phi^{(1)} = \hat{\phi}^{(1)}, \\
&\bar{\sigma}^{(2)} = -n_i\bar{D}_i^{(2)} \text{ or } \quad \phi^{(2)} = \hat{\phi}^{(2)}.
\end{aligned}
\tag{35}
$$

According to $(8)_{2,3}$, stress components $T_{a2}^{(0)}$ and $\bar{T}_{a2}^{(1)}$ are related to transverse shear stress $T_{a2}$ by:

$$
\begin{aligned}
T_{a2}^{(0)} &= \int_{-1}^{1} T_{a2}d\psi, \\
\bar{T}_{a2}^{(1)} &= \int_{-1}^{1} T_{a2}\cos(\frac{\pi}{2}\psi)d\psi.
\end{aligned}
\tag{36}
$$

It is well-known that the distribution of $T_{a2}$ across the thickness is a parabolic function, i.e., $T_{a2} = c(1-\psi^2)$, for a plate which is free of tangential tractions at faces $\psi = \pm 1$ and under statical bending or at low-frequency flexural vibrations. Substitution of the distribution into (36) leads to:

$$
T_{a2}^{(0)} = \frac{\pi^3}{24}\bar{T}_{a2}^{(1)}, \tag{37}
$$

which agrees with (33) of [7]. By inserting (37) into the second equation (25) (for $j = 2$), which is the equation of the lowest order for flexural vibrations, we have the modified equation of motion for the transverse displacement $u_2^{(0)}$:

$$
\frac{\pi^3}{24}\bar{T}_{a2,a}^{(1)} + \frac{1}{b}F_j^{(0)} = \rho^{(0)}\ddot{u}_2^{(0)} + \rho^{(1)}\ddot{u}_2^{(1)}. \tag{38}
$$

It is shown that the 2-D equations (25) with the modification (38) yield the exact asymptotic dispersion relation from 3-D theory for flexural vibration of isotropic homogeneous plate as both frequency and wave number approaching zero [12]. It also has been observed in [7] that the modified system of first-order 2-D equations gives prediction of the frequency spectrum for AT-cut quartz closer to the experimental data by Koga and Fukuyo [13].

Substitution of (34) into (28) and then into (25) and (38) leads to the first-order governing equations on mechanical displacements and electric potentials. For the composite plate consisting of an AT-cut quartz and two identical electrodes shown in Fig. 2, the equations are greatly reduced. Furthermore, for the $x_1$-varying modes, the essentially symmetric modes (extensional, thickness-stretch, and thickness-twist) and the essentially antisymmetric modes (flexural, thickness-shear, and face-shear) are uncoupled from each other. The governing equations for the essentially antisymmetric modes, which can be piezoelectrically excited and are of practical interests, are:

$$\begin{aligned}
&\frac{\pi^3}{24}\left(c_{65}^{(\bar{1}0)}u_{3,11}^{(0)}+\frac{\pi}{2b}c_{66}^{(\bar{1}\bar{1})}u_{1,1}^{(1)}-\frac{\pi}{b}\bar{e}_{26}^{(\bar{2}\bar{1})}\phi_{,1}^{(2)}\right)\\
&\qquad+\frac{1}{b}F_2^{(0)}=\rho^{(0)}\ddot{u}_2^{(0)},\\
&c_{55}^{(00)}u_{3,11}^{(0)}+\frac{\pi}{2b}c_{56}^{(0\bar{1})}u_{1,1}^{(1)}-\frac{\pi}{b}\bar{e}_{25}^{(\bar{2}0)}\phi_{,1}^{(2)}+\frac{1}{b}F_3^{(0)}=\rho^{(0)}\ddot{u}_3^{(0)},\\
&-c_{11}^{(1d)}bu_{2,111}^{(0)}+c_{11}^{(11)}u_{1,11}^{(1)}-\frac{\pi}{2b}c_{65}^{(\bar{1}0)}u_{3,1}^{(0)}-\frac{\pi^2}{4b^2}c_{66}^{(\bar{1}\bar{1})}u_1^{(1)}\\
&\qquad+\bar{e}_{11}^{(21)}\phi_{,11}^{(2)}+\frac{\pi^2}{2b^2}\bar{e}_{26}^{(\bar{2}\bar{1})}\phi^{(2)}-\frac{\pi}{2b}\bar{e}_{26}^{(\bar{0}\bar{1})}\frac{\bar{V}_1}{b_q}+\frac{1}{b}F_1^{(1)}\\
&\qquad=\frac{1}{2}\left(\rho^{(0)}+\rho^{(2)}\right)\ddot{u}_1^{(1)}-\hat{\rho}^{(1)}b\ddot{u}_{2,1}^{(0)},\\
&-e_{11}^{(\bar{2}d)}bu_{2,111}^{(0)}+e_{11}^{(\bar{2}1)}u_{1,11}^{(1)}+\frac{\pi}{b}e_{25}^{(20)}u_{3,1}^{(0)}+\frac{\pi^2}{2b^2}e_{26}^{(2\bar{1})}u_1^{(1)}\\
&\qquad-\epsilon_{11}^{(\bar{2}2)}\phi_{,11}^{(2)}+\frac{\pi^2}{b^2}\epsilon_{22}^{(2\bar{2})}\phi^{(2)}-\frac{\pi}{b}\epsilon_{22}^{(2\bar{0})}\frac{\bar{V}_1}{b_q}=0,
\end{aligned}\tag{39}$$

where

$$\begin{aligned}
&c_{pq}^{(00)}=c_{pq}^{(0)},c_{pq}^{(0\bar{1})}=c_{pq}^{(\bar{1}0)}=\bar{c}_{pq}^{(1)},\\
&c_{pq}^{(\bar{1}\bar{1})}=\frac{1}{2}(c_{pq}^{(0)}-c_{pq}^{(2)}),c_{pq}^{(1d)}=\hat{c}_{pq}^{(1)}-\frac{\bar{c}_{p2}^{(1)}+\bar{c}_{p2}^{(3)}}{\bar{c}_{22}^{(1)}+\bar{c}_{22}^{(3)}}\hat{c}_{2q}^{(1)},\\
&c_{pq}^{(11)}=\frac{1}{2}\left(c_{pq}^{(0)}+c_{pq}^{(2)}\right)-\frac{1}{2}\frac{\bar{c}_{p2}^{(1)}+\bar{c}_{p2}^{(3)}}{\bar{c}_{22}^{(1)}+\bar{c}_{22}^{(3)}}\left(c_{2q}^{(0)}+c_{2q}^{(2)}\right);
\end{aligned}\tag{40}$$

$$\begin{aligned}
&\bar{e}_{ip}^{(21)}=\frac{1}{2}\left(\bar{e}_{ip}^{(1)}+\bar{e}_{ip}^{(3)}\right)-\frac{1}{2}\frac{\bar{c}_{p2}^{(1)}+\bar{c}_{p2}^{(3)}}{\bar{c}_{22}^{(1)}+\bar{c}_{22}^{(3)}}\left(\bar{e}_{i2}^{(1)}+\bar{e}_{i2}^{(3)}\right),\\
&\bar{e}_{ip}^{(\bar{2}0)}=e_{ip}^{(20)}=e_{ip}^{(2)},\bar{e}_{ip}^{(\bar{0}\bar{1})}=\bar{e}_{ip}^{(1)},\\
&\bar{e}_{ip}^{(\bar{2}\bar{1})}=e_{ip}^{(2\bar{1})}=\frac{1}{2}\left(\bar{e}_{ip}^{(3)}-\bar{e}_{ip}^{(1)}\right),\\
&e_{ip}^{(\bar{2}d)}=\tilde{e}_{ip}^{(2)}-\frac{(e_{i2}^{(0)}-e_{i2}^{(4)})\hat{c}_{2p}^{(1)}}{\bar{c}_{22}^{(1)}+\bar{c}_{22}^{(3)}},\\
&e_{ip}^{(\bar{2}1)}=\frac{1}{2}\left(\bar{e}_{ip}^{(1)}+\bar{e}_{ip}^{(3)}\right)-\frac{1}{2}\left(e_{i2}^{(0)}-e_{i2}^{(4)}\right)\frac{c_{2p}^{(0)}+c_{2p}^{(2)}}{\bar{c}_{22}^{(1)}+\bar{c}_{22}^{(3)}};
\end{aligned}\tag{41}$$

$$\begin{aligned}
&\epsilon_{ij}^{(\bar{2}\bar{2})}=\frac{1}{2}\left(\epsilon_{ij}^{(0)}-\epsilon_{ij}^{(4)}\right)+\frac{1}{2}\left(e_{i2}^{(0)}-e_{i2}^{(4)}\right)\frac{\bar{e}_{j2}^{(1)}+\bar{e}_{j2}^{(3)}}{\bar{c}_{22}^{(1)}+\bar{c}_{22}^{(3)}},\\
&\epsilon_{ij}^{(2\bar{2})}=\frac{1}{2}\left(\epsilon_{ij}^{(0)}+\epsilon_{ij}^{(4)}\right),\epsilon_{ij}^{(2\bar{0})}=\epsilon_{ij}^{(2)},
\end{aligned}\tag{42}$$

and $c_{pq}^{(n)}$, $\bar{c}_{pq}^{(n)}$, $\hat{c}_{pq}^{(n)}$, $e_{ip}^{(n)}$, $\bar{e}_{ip}^{(n)}$, $\tilde{e}_{ip}^{(n)}$, and $\epsilon_{ij}^{(n)}$ are obtained from (23). For the quartz plate with identical electrodes, we have:

$$\begin{aligned}
&\mathcal{M}^{(0)}=2\mathcal{M}_q\frac{1+r_tr_{\mathcal{M}}}{1+r_t},\\
&\mathcal{M}^{(2)}=-\frac{2}{\pi}\mathcal{M}_q(1-r_{\mathcal{M}})\sin 2\alpha,\\
&\mathcal{M}^{(4)}=-\frac{1}{\pi}\mathcal{M}_q(1-r_{\mathcal{M}})\sin 4\alpha,\\
&\tilde{\mathcal{M}}^{(1)}=\frac{4}{\pi}\mathcal{M}_q\left[r_{\mathcal{M}}+(1-r_{\mathcal{M}})\sin\alpha\right],\\
&\tilde{\mathcal{M}}^{(3)}=\frac{4}{3\pi}\mathcal{M}_q\left[r_{\mathcal{M}}-(1-r_{\mathcal{M}})\sin 3\alpha\right],\\
&\hat{\mathcal{M}}^{(1)}=\frac{8}{\pi^2}\mathcal{M}_q\left[r_{\mathcal{M}}+(1-r_{\mathcal{M}})(\sin\alpha-\alpha\cos\alpha)\right],\\
&\tilde{\mathcal{M}}^{(2)}=\frac{2}{\pi^2}\mathcal{M}_q\left[\pi r_{\mathcal{M}}+(1-r_{\mathcal{M}})(\sin 2\alpha-2\alpha\cos 2\alpha)\right],
\end{aligned}\tag{43}$$

where

$$\alpha=\frac{\pi}{2(1+r_t)},r_t=\frac{2b_e}{b_q},r_{\mathcal{M}}=\frac{\mathcal{M}_e}{\mathcal{M}_q},\tag{44}$$

and $r_t$ is the ratio of the thickness of electrode to that of quartz, $\mathcal{M}_q$ and $\mathcal{M}_e$ represent the material properties (including mass density) of quartz and electrode, respectively.

We note that the ratio of the mass of electrodes to that of quartz per unit plate area, $R$, is related to $r_t$ and the density ratio $r_\rho$,

$$R=r_tr_\rho,r_\rho=\frac{\rho'}{\rho},\tag{45}$$

where $\rho'$ and $\rho$ are the mass densities of electrode and quartz, respectively.

By substituting (43) into (40)–(42), we see that the material coefficients in the governing equations (39) contain electrode effects through the explicit expressions in terms of the thickness ratio $r_t$, density ratio $r_\rho$ (or mass ratio $R$), and stiffness ratios $r_c$.

## IV. Dispersion Relations

For the $TS_1-F_1-FS_1$ vibrations, we let:

$$\begin{aligned}
u_2^{(0)}&=A_1\sin(\xi x_1)e^{i\omega t},\\
u_3^{(0)}&=A_2\sin(\xi x_1)e^{i\omega t},\\
u_1^{(1)}&=A_3\cos(\xi x_1)e^{i\omega t},\\
\phi^{(2)}&=A_4\sqrt{\frac{c_{66}}{\epsilon_{22}}}\cos(\xi x_1)e^{i\omega t}.
\end{aligned}\tag{46}$$

By substituting (46) into (39) and setting $F_2^{(0)}$, $F_3^{(0)}$, $F_1^{(1)}$, and $\bar{V}_1$ to zero for free vibrations and shorted faces, we obtain:

$$\sum_{j=1}^{4}Q_{ij}(\Omega,X)A_j=0,\quad i,j=1,\cdots,4,\tag{47}$$

$$\begin{bmatrix} \bar{r}_\rho\Omega^2 & -\frac{\pi^3}{24}\frac{c_{65}^{(\bar{1}0)}}{c_{66}}X^2 & -\frac{\pi^3}{24}\frac{c_{66}^{(\bar{1}\bar{1})}}{\bar{r}_t c_{66}}X & \frac{\pi^3\bar{e}_{26}^{(\bar{2}\bar{1})}}{12\bar{r}_t\sqrt{c_{66}\epsilon_{22}}}X \\ 0 & \bar{r}_\rho\Omega^2 - \frac{c_{55}^{(00)}}{c_{66}}X^2 & -\frac{c_{56}^{(0\bar{1})}}{\bar{r}_t c_{66}}X & \frac{2\bar{e}_{25}^{(\bar{2}0)}}{\bar{r}_t\sqrt{c_{66}\epsilon_{22}}}X \\ \frac{\pi}{2}\bar{r}_t X\left(\frac{c_{11}^{(1d)}}{c_{66}}X^2 - \hat{r}_\rho\Omega^2\right) & -\frac{c_{65}^{(\bar{1}0)}}{\bar{r}_t c_{66}}X & \tilde{r}_\rho\Omega^2 - \frac{c_{11}^{(11)}}{c_{66}}X^2 - \frac{c_{66}^{(\bar{1}\bar{1})}}{\bar{r}_t^2 c_{66}} & -\frac{\bar{e}_{11}^{(21)}}{\sqrt{c_{66}\epsilon_{22}}}X^2 + \frac{2\bar{e}_{26}^{(\bar{2}\bar{1})}}{\bar{r}_t^2\sqrt{c_{66}\epsilon_{22}}} \\ \frac{\pi\bar{r}_t e_{11}^{(\bar{2}d)}}{2\sqrt{c_{66}\epsilon_{22}}}X^3 & \frac{2e_{25}^{(20)}}{\bar{r}_t\sqrt{c_{66}\epsilon_{22}}}X & -\frac{e_{11}^{(\bar{2}1)}}{\sqrt{c_{66}\epsilon_{22}}}X^2 + \frac{2e_{26}^{(2\bar{1})}}{\bar{r}_t^2\sqrt{c_{66}\epsilon_{22}}} & \frac{\epsilon_{11}^{(\bar{2}\bar{2})}}{\epsilon_{22}}X^2 + \frac{4\epsilon_{22}^{(2\bar{2})}}{\bar{r}_t^2\epsilon_{22}} \end{bmatrix} \tag{48}$$

where the coefficient matrix $[Q_{ij}]$ is [see (48); above] and

$$\Omega = \frac{\omega}{\frac{\pi}{2b_q}\sqrt{\frac{c_{66}}{\rho}}}, X = \frac{\xi}{\frac{\pi}{2b_q}},$$
$$\bar{r}_t = \frac{b}{b_q} = 1 + r_t, \bar{r}_\rho = \frac{\rho^{(0)}}{\rho}, \tag{49}$$
$$\hat{r}_\rho = \frac{\hat{\rho}^{(1)}}{\rho}, \tilde{r}_\rho = \frac{\rho^{(0)} + \rho^{(2)}}{2\rho}.$$

For nontrivial solutions of (47), we have:

$$\det[Q_{ij}(\Omega, X)] = 0, \tag{50}$$

which gives the dispersion relations for the $TS_1$-$F_1$-$FS_1$ vibrations of the composite plate.

By setting $X = 0$ in (50) and solving for $\Omega$, we obtain:

$$\Omega_c = \frac{1}{\bar{r}_t}\sqrt{\frac{1}{\tilde{r}_\rho}\left(\frac{c_{66}^{(\bar{1}\bar{1})}}{c_{66}} + \frac{\bar{e}_{26}^{(\bar{2}\bar{1})}e_{26}^{(2\bar{1})}}{c_{66}\epsilon_{22}^{(2\bar{2})}}\right)}, \tag{51}$$

which is the cut-off frequency of the fundamental thickness-shear mode. The present formula may be compared with:

$$\Omega_c = \sqrt{\frac{1}{1 + 2r_\rho r_t}\left(1 + \frac{16}{9\pi^2}\frac{e_{26}^2}{c_{66}\epsilon_{22}}\right)}, \tag{52}$$

which is obtained from the 2-D equations of [7] for which only the effect of electrode mass is taken into account. The exact frequency for the fundamental TS mode can be computed as the lowest root of (87), which is obtained from the solutions of 3-D equations given in the Appendix. Cut-off frequencies of an AT-cut quartz plate with electrodes of gold, silver, and aluminum are computed as functions of $r_t$ from (51), (52), and (87) and are shown in Fig. 3 for comparison. Bechmann's values of the material constants of quartz [14] are used for computation. The electrodes are assumed to be isotropic and perfect conducting, for which the piezoelectric coefficients and dielectric constants are set to zero, and the mass density and elastic stiffness are obtained from [15].

From Fig. 3, we see that the present 2-D equations, including both stiffness and mass effects of electrodes, give closer prediction for the cut-off frequencies than the 2-D equations including only mass effect, especially for large thickness ratio $r_t$.

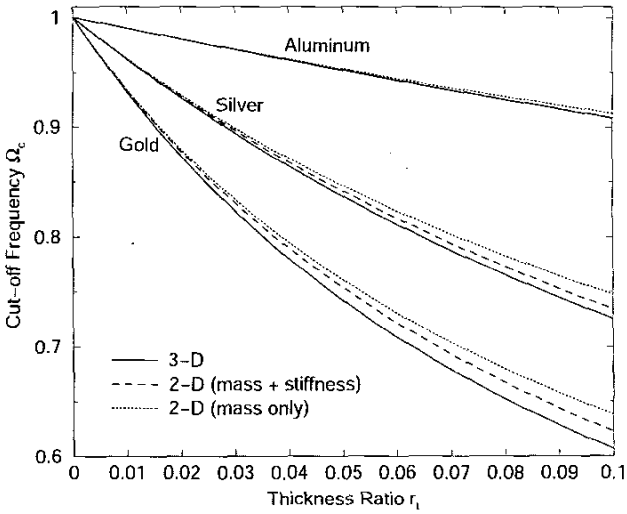


Fig. 3. Comparisons of the thickness-shear cut-off frequencies of an AT-cut quartz plate as a function of the thickness ratio ($r_t = 2b_e/b_q$) predicted by the 3-D equations (solid lines), present 2-D equations (dashed lines), and 2-D equations with mass effect only (dotted lines).

Dispersion curves are then calculated from (50) for composite plates with gold and aluminum electrodes of mass ratios $R = 0.05$, as shown in Fig. 4. For comparison, dispersion curves are also calculated from (86), which is obtained from the solutions of 3-D equations given in the Appendix, and plotted in Fig. 5. It may be seen from Figs. 4 and 5 that the dispersion curves of the $TS_1$, $F_1$, and $FS_1$ modes predicted from the present 2-D equations agree closely with the corresponding ones from the 3-D equations for different electrodes, without introducing any correction factors.

## V. Frequency Spectra

For a given value of frequency $\Omega$, (50) yields four roots of wave numbers: $X_k$ or $\xi_k$ with $k = 1, \cdots, 4$, and for each

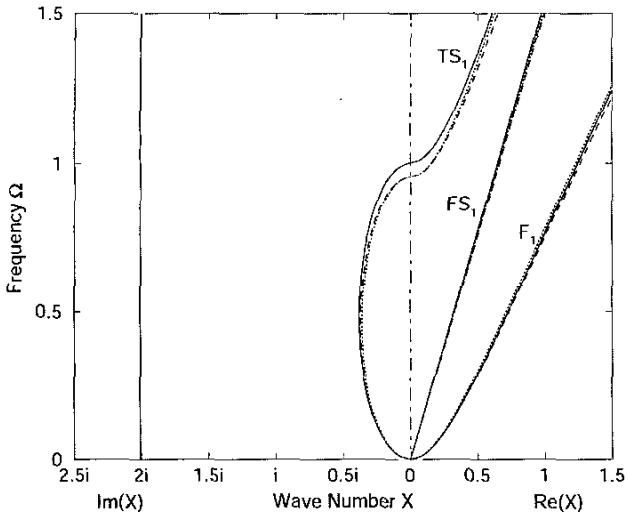


Fig. 4. Dispersion curves computed from the present 2-D equations for AT-cut quartz plates: solid lines for plate without electrodes ($R = 0$), dashed lines for plate with gold electrodes ($R = 0.05$), and dotted lines for plate with aluminum electrodes ($R = 0.05$).

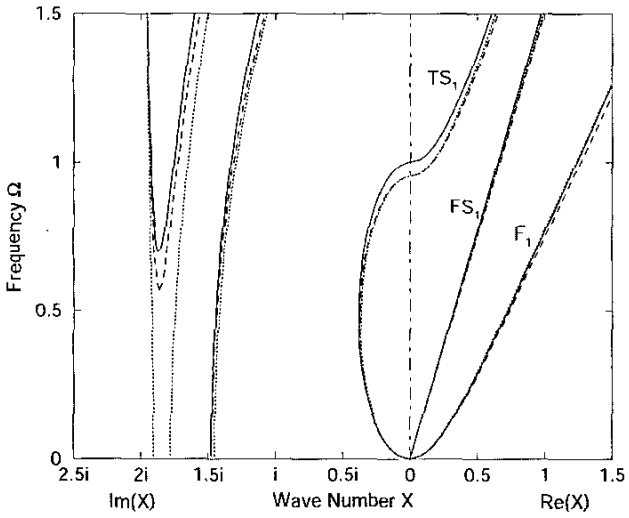


Fig. 5. Dispersion curves computed from the 3-D equations for AT-cut quartz plates: solid lines for plate without electrodes ($R = 0$), dashed lines for plate with gold electrodes ($R = 0.05$), and dotted lines for plate with aluminum electrodes ($R = 0.05$).

root the amplitude ratios $\alpha_{jk}$ satisfy:

$$\sum_{j=1}^{4} Q_{ij}(\Omega, X_k)\alpha_{jk} = 0, \quad i,k = 1,\cdots,4. \tag{53}$$

The general solution for free vibrations of the composite plate takes the form:

$$\begin{aligned} u_2^{(0)} &= \sum_{j=1}^{4} \alpha_{1j} B_j \sin(\xi_j x_1) e^{i\omega t}, \\ u_3^{(0)} &= \sum_{j=1}^{4} \alpha_{2j} B_j \sin(\xi_j x_1) e^{i\omega t}, \\ u_1^{(1)} &= \sum_{j=1}^{4} \alpha_{3j} B_j \cos(\xi_j x_1) e^{i\omega t}, \\ \phi^{(2)} &= \sqrt{\frac{c_{66}}{\epsilon_{22}}} \sum_{j=1}^{4} \alpha_{4j} B_j \cos(\xi_j x_1) e^{i\omega t}. \end{aligned} \tag{54}$$

By inserting (37) into (35), we obtain the edge conditions for $TS_1 - F_1 - FS_1$ vibrations of an infinite strip with a pair of traction-free and charge-free edges at $x_1 = \pm a$:

$$\bar{T}_6^{(1)} = T_5^{(0)} = T_1^{(1)} = \bar{D}_1^{(2)} = 0. \tag{55}$$

The stresses and charge density in (55) expressed in terms of $u_i^{(n)}$ and $\phi^{(n)}$ are obtained by substituting (34) into (28),

$$\begin{aligned} \bar{T}_6^{(1)} &= c_{65}^{(\bar{1}0)} u_{3,1}^{(0)} + \frac{\pi}{2b} c_{66}^{(\bar{1}\bar{1})} u_1^{(1)} - \frac{\pi}{b} \bar{e}_{26}^{(\bar{2}\bar{1})} \phi^{(2)}, \\ T_5^{(0)} &= c_{55}^{(00)} u_{3,1}^{(0)} + \frac{\pi}{2b} c_{56}^{(0\bar{1})} u_1^{(1)} - \frac{\pi}{b} \bar{e}_{25}^{(\bar{2}0)} \phi^{(2)}, \\ T_1^{(1)} &= -c_{11}^{(1d)} b u_{2,11}^{(0)} + c_{11}^{(11)} u_{1,1}^{(1)} + \bar{e}_{11}^{(21)} \phi_{,1}^{(2)}, \\ \bar{D}_1^{(2)} &= -e_{11}^{(\bar{2}d)} b u_{2,11}^{(0)} + e_{11}^{(\bar{2}1)} u_{1,1}^{(1)} - \epsilon_{11}^{(\bar{2}2)} \phi_{,1}^{(2)}. \end{aligned} \tag{56}$$

Substitution of (54) into (56) and then into (55) leads to

$$\sum_{j=1}^{4} M_{ij} B_j = 0, \quad i = 1,\cdots,4, \tag{57}$$

where [see (58); next page].

Vanishing of the determinant of the matrix $M_{ij}$ gives the frequency equation for the free vibrations of a quartz strip with two identical electrodes,

$$\det\left[M_{ij}\left(\Omega, \frac{a}{b_q}, R, r_{\mathcal{M}}\right)\right] = 0. \tag{59}$$

The resonance frequency is computed from (59) as a function of $a/b_q$, the length-to-thickness ratio of the quartz plate. For plates without electrodes (i.e., $R = 0$), the spectrum reduces to that obtained in [7] for homogeneous plates, as shown by the dotted lines in Fig. 6. The solid lines in Fig. 6 denote the spectrum of the AT-cut quartz plates with gold electrodes and for mass ratio $R = 0.005$. Similar computations are made for AT-cut quartz with aluminum electrodes; the results are shown in Fig. 7.

Fig. 8 shows the predominantly $TS_1 - 1$ and $F_1 - 46$ branch of the spectrum in Fig. 6 with different mass ratios of gold electrodes. It may be seen from Figs. 6 and 8

$$
\begin{aligned}
M_{1j} &= \left( \frac{c_{65}^{(\bar{1}0)}}{c_{66}} \bar{r}_t \alpha_{2j} X_j + \frac{c_{66}^{(\bar{1}\bar{1})}}{c_{66}} \alpha_{3j} - \frac{2\bar{e}_{26}^{(\bar{2}\bar{1})}}{\sqrt{c_{66}\epsilon_{22}}} \alpha_{4j} \right) \cos(\xi_j a), \\
M_{2j} &= \left( \frac{c_{55}^{(00)}}{c_{66}} \bar{r}_t \alpha_{2j} X_j + \frac{c_{56}^{(0\bar{1})}}{c_{66}} \alpha_{3j} - \frac{2\bar{e}_{25}^{(\bar{2}0)}}{\sqrt{c_{66}\epsilon_{22}}} \alpha_{4j} \right) \cos(\xi_j a), \\
M_{3j} &= \left( \frac{\pi c_{11}^{(1d)}}{2c_{66}} \bar{r}_t \alpha_{1j} X_j^2 - \frac{c_{11}^{(11)}}{c_{66}} \alpha_{3j} X_j - \frac{\bar{e}_{11}^{(21)}}{\sqrt{c_{66}\epsilon_{22}}} \alpha_{4j} X_j \right) \sin(\xi_j a), \\
M_{4j} &= \left( \frac{\pi e_{11}^{(\bar{2}d)}}{2\sqrt{c_{66}\epsilon_{22}}} \bar{r}_t \alpha_{1j} X_j^2 - \frac{e_{11}^{(\bar{2}1)}}{\sqrt{c_{66}\epsilon_{22}}} \alpha_{3j} X_j + \frac{\epsilon_{11}^{(\bar{2}2)}}{\epsilon_{22}} \alpha_{4j} X_j \right) \sin(\xi_j a)
\end{aligned}
\tag{58}
$$

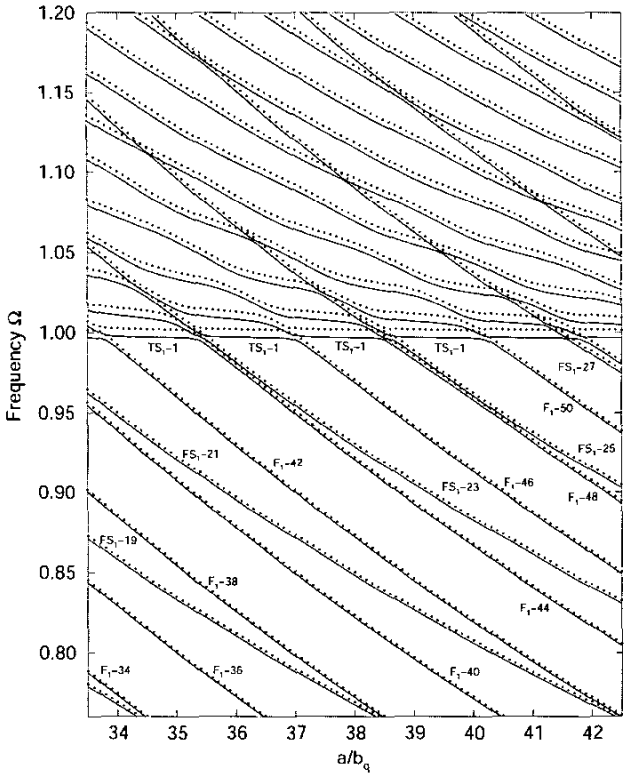


Fig. 6. Resonance frequency $\Omega$ vs. length-to-thickness ratio $a/b_q$ for AT-cut quartz plates, solid lines for plates with gold electrodes ($R = 0.005$) and dotted lines for plates without electrodes ($R = 0$).

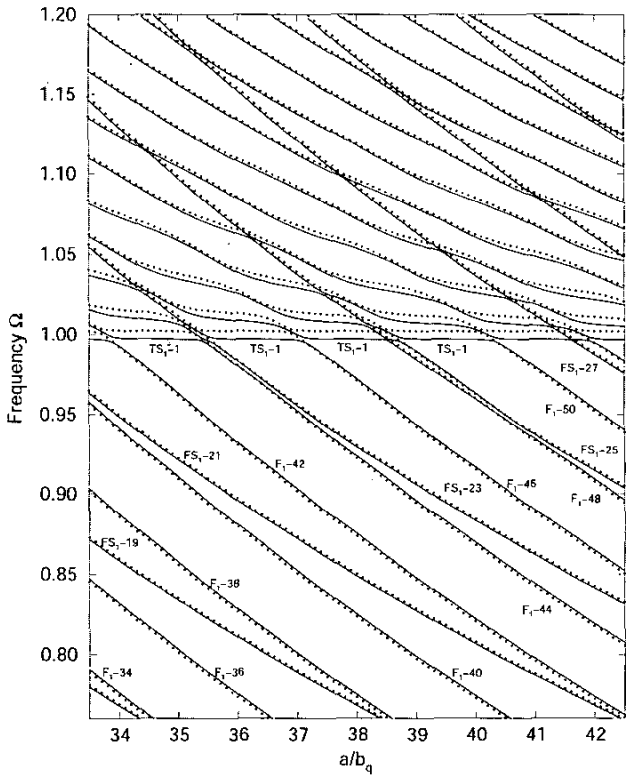


Fig. 7. Resonance frequency $\Omega$ vs. length-to-thickness ratio $a/b_q$ for AT-cut quartz plates, solid lines for plates with aluminum electrodes ($R = 0.005$) and dotted lines for plates without electrodes ($R = 0$).

that, for a quartz plate with gold electrodes, the resonance frequencies of all three modes are decreasing as the mass ratio increases; but, the amount of the frequency changes for the $TS_1$ mode is much greater than those for $F_1$ and $FS_1$ modes.

Frequency spectrum of $\Omega$ vs. $R$ is computed from (59) for a quartz plate with aluminum electrodes and for $a/b_q = 36.5$, and it is shown in Fig. 9. It is seen from Fig. 9 that the mass ratio $R$ can affect the strength of coupling among the vibrational modes. From Fig. 7 and 9, we see that resonance frequencies of the $TS_1$ and $FS_1$ modes decrease and those of $F_1$ modes increase as the mass ratio of aluminum electrodes increases.

Therefore, it is seen from (51) or Fig. 3 that the frequency of $TS_1$ mode decreases as R increases for plates with gold, silver, or aluminum electrodes. For the $F_1$ mode, it seems that the increase or decrease of the frequency depends on whether the extensional wave velocity in the electrode is greater or less than that in the quartz, i.e.,

$$
\left( \frac{\Omega - \Omega_0}{\Omega_0} \right)_{F_1} \propto \sqrt{\frac{c'_{11}/\rho'}{c_{11}/\rho}} - 1, \tag{60}
$$

where $\Omega_0$ is the frequency for the plate without electrodes.

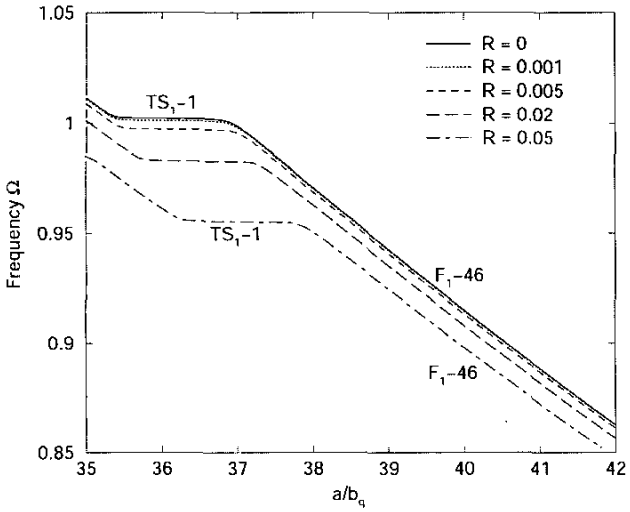


Fig. 8. Effects of gold electrodes on the predominantly thickness-shear and flexural branches of the frequency spectrum of AT-cut quartz plates with various mass ratio $R$.

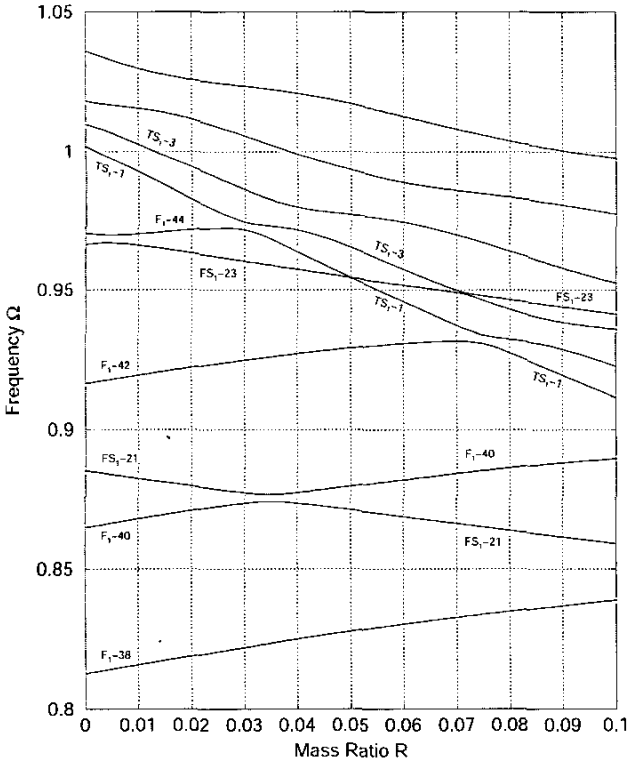


Fig. 9. Resonance frequency $\Omega$ vs. mass ratio $R$ for AT-cut quartz plates with aluminum electrodes and $a/b_q = 36.5$.

Similarly, for the face-shear mode,

$$\left(\frac{\Omega-\Omega_0}{\Omega_0}\right)_{FS_1} \propto \sqrt{\frac{c'_{55}/\rho'}{c_{55}/\rho}} - 1, \tag{61}$$

which agrees with Mindlin's observations in [1].

## Appendix A
## 3-D Equations and Solutions

Consider straight-crested waves propagating in the $x_1$ direction of an infinite composite plate as shown in Fig. 2. We let:

$$u_i = u_i(x_1, x_2, t), \phi = \phi(x_1, x_2, t), i = 1, 2, 3. \tag{62}$$

Constitutive equations for the AT-cut quartz ($-b_q < x_2 < b_q$) are:

$$\begin{aligned}
T_1 &= c_{11}u_{1,1} + c_{12}u_{2,2} + c_{14}u_{3,2} + e_{11}\phi_{,1},\\
T_2 &= c_{21}u_{1,1} + c_{22}u_{2,2} + c_{24}u_{3,2} + e_{12}\phi_{,1},\\
T_3 &= c_{31}u_{1,1} + c_{32}u_{2,2} + c_{34}u_{3,2} + e_{13}\phi_{,1},\\
T_4 &= c_{41}u_{1,1} + c_{42}u_{2,2} + c_{44}u_{3,2} + e_{14}\phi_{,1},\\
T_5 &= c_{55}u_{3,1} + c_{56}(u_{1,2} + u_{2,1}) + e_{25}\phi_{,2},\\
T_6 &= c_{65}u_{3,1} + c_{66}(u_{1,2} + u_{2,1}) + e_{26}\phi_{,2},\\
D_1 &= e_{11}u_{1,1} + e_{12}u_{2,2} + e_{14}u_{3,2} - \epsilon_{11}\phi_{,1},\\
D_2 &= e_{25}u_{3,1} + e_{26}(u_{1,2} + u_{2,1}) - \epsilon_{22}\phi_{,2},\\
D_3 &= e_{35}u_{3,1} + e_{36}(u_{1,2} + u_{2,1}) - \epsilon_{32}\phi_{,2},
\end{aligned} \tag{63}$$

and for isotropic electrodes ($-b < x_2 < -b_q$ or $b_q < x_2 < b$),

$$\begin{aligned}
T_1 &= c'_{11}u_{1,1} + c'_{12}u_{2,2},\\
T_2 &= c'_{21}u_{1,1} + c'_{22}u_{2,2},\\
T_3 &= c'_{31}u_{1,1} + c'_{32}u_{2,2},\\
T_4 &= c'_{44}u_{3,2},\\
T_5 &= c'_{55}u_{3,1},\\
T_6 &= c'_{66}(u_{1,2} + u_{2,1}).
\end{aligned} \tag{64}$$

Substitution of (63) and (64) into $(1)_1$ leads to the governing equations of $u_i$ and $\phi$, for quartz:

$$\begin{aligned}
&c_{11}u_{1,11} + c_{66}u_{1,22} + (c_{12} + c_{66})u_{2,12} + (c_{14} + c_{56})u_{3,12}\\
&\quad + e_{11}\phi_{,11} + e_{26}\phi_{,22} = \rho\ddot{u}_1,\\
&(c_{12} + c_{66})u_{1,12} + c_{66}u_{2,11} + c_{22}u_{2,22} + c_{56}u_{3,11}\\
&\quad + c_{24}u_{3,22} + (e_{12} + e_{26})\phi_{,12} = \rho\ddot{u}_2,\\
&(c_{14} + c_{56})u_{1,12} + c_{56}u_{2,11} + c_{24}u_{2,22} + c_{55}u_{3,11}\\
&\quad + c_{44}u_{3,22} + (e_{14} + e_{25})\phi_{,12} = \rho\ddot{u}_3,\\
&e_{11}u_{1,11} + e_{26}u_{1,22} + (e_{12} + e_{26})u_{2,12} + (e_{14} + e_{25})u_{3,12}\\
&\quad - \epsilon_{11}\phi_{,11} - \epsilon_{22}\phi_{,22} = 0,
\end{aligned} \tag{65}$$

and for electrodes,

$$\begin{aligned}
&c'_{11}u_{1,11} + c'_{66}u_{1,22} + (c'_{12} + c'_{66})u_{2,12} = \rho'\ddot{u}_1,\\
&\quad (c'_{12} + c'_{66})u_{1,12} + c'_{66}u_{2,11} + c'_{22}u_{2,22} = \rho'\ddot{u}_2,\\
&c'_{55}u_{3,11} + c'_{44}u_{3,22} = \rho'\ddot{u}_3.
\end{aligned} \tag{66}$$

For $u_i$ and $\phi$ antisymmetric with respect to the middle plane of the plate, we let, for quartz $(-b_q < x_2 < b_q)$,

$$\begin{aligned} u_1 &= A_1 \sin(\eta x_2) e^{i(\xi x_1 - \omega t)}, \\ u_2 &= iA_2 \cos(\eta x_2) e^{i(\xi x_1 - \omega t)}, \\ u_3 &= iA_3 \cos(\eta x_2) e^{i(\xi x_1 - \omega t)}, \\ \phi &= \sqrt{\frac{c_{66}}{\epsilon_{22}}} A_4 \sin(\eta x_2) e^{i(\xi x_1 - \omega t)}, \end{aligned} \tag{67}$$

and for electrodes

$$\begin{aligned} u_1 &= [A_1' \sin(\eta' x_2) \pm B_1' \cos(\eta' x_2)] e^{i(\xi x_1 - \omega t)}, \\ u_2 &= i[A_2' \cos(\eta' x_2) \mp B_2' \sin(\eta' x_2)] e^{i(\xi x_1 - \omega t)}, \\ u_3 &= i[A_3' \cos(\eta' x_2) \mp B_3' \sin(\eta' x_2)] e^{i(\xi x_1 - \omega t)}, \end{aligned} \tag{68}$$

where the upper and lower signs are for the upper and lower electrodes, respectively.

Upon substituting (67) into (65), we have:

$$\sum_{j=1}^{4} Q_{ij}(\Omega, X, Y) A_j = 0, \quad i, j = 1, \cdots, 4, \tag{69}$$

where

$$\begin{aligned} Q_{11} &= \Omega^2 - \bar{c}_{11} X^2 - Y^2, \\ Q_{22} &= \Omega^2 - X^2 - \bar{c}_{22} Y^2, \\ Q_{33} &= \Omega^2 - \bar{c}_{55} X^2 - \bar{c}_{44} Y^2, \\ Q_{44} &= \bar{\epsilon}_{11} X^2 + Y^2, \\ Q_{12} &= Q_{21} = (1 + \bar{c}_{12}) XY, \\ Q_{13} &= Q_{31} = (\bar{e}_{14} + \bar{c}_{56}) XY, \\ Q_{23} &= Q_{32} = -\bar{c}_{56} X^2 - \bar{c}_{24} Y^2, \\ Q_{14} &= Q_{41} = -\bar{e}_{11} X^2 - \bar{e}_{26} Y^2, \\ Q_{24} &= Q_{42} = (\bar{e}_{12} + \bar{e}_{26}) XY, \\ Q_{34} &= Q_{43} = (\bar{e}_{14} + \bar{e}_{25}) XY, \end{aligned} \tag{70}$$

and

$$\begin{aligned} &\Omega = \frac{\omega}{\frac{\pi}{2b_q}\sqrt{\frac{c_{66}}{\rho}}}, X = \frac{2}{\pi}\xi b_q, Y = \frac{2}{\pi}\eta b_q, \\ &\bar{c}_{pq} = \frac{c_{pq}}{c_{66}}, \bar{e}_{ip} = \frac{e_{ip}}{\sqrt{c_{66}\epsilon_{22}}}, \bar{\epsilon}_{ij} = \frac{\epsilon_{ij}}{\epsilon_{22}}. \end{aligned} \tag{71}$$

The vanishing of the determinant

$$\det[Q_{ij}(\Omega, X, Y)] = 0, \tag{72}$$

gives a fourth-order polynomial equation of $Y^2$. For given frequency $\Omega$ and wave number $X$, (72) yields four roots, $Y_k$ or $\eta_k$, $k = 1, \cdots, 4$. Thus, the general solution for the displacement and potential in the quartz are, for $-b_q < x_2 < b_q$:

$$\begin{aligned} u_1 &= \sum_{j=1}^{4} \alpha_{1j} A_j \sin(\eta_j x_2) e^{i(\xi x_1 - \omega t)}, \\ u_2 &= i \sum_{j=1}^{4} \alpha_{2j} A_j \cos(\eta_j x_2) e^{i(\xi x_1 - \omega t)}, \\ u_3 &= i \sum_{j=1}^{4} \alpha_{3j} A_j \cos(\eta_j x_2) e^{i(\xi x_1 - \omega t)}, \\ \phi &= \sqrt{\frac{c_{66}}{\epsilon_{22}}} \sum_{j=1}^{4} \alpha_{4j} A_j \sin(\eta_j x_2) e^{i(\xi x_1 - \omega t)}, \end{aligned} \tag{73}$$

where $\alpha_{kj}$ satisfy:

$$\sum_{k=1}^{4} Q_{ik}(\Omega, X, Y_j) \alpha_{kj} = 0, \quad i, j = 1, \cdots, 4. \tag{74}$$

Similarly, for the electrodes, substitution of (68) into (66) leads to:

$$\sum_{s=1}^{3} Q_{rs}'(\Omega, X, Y') A_s' = \sum_{s=1}^{3} Q_{rs}'(\Omega, X, Y') B_s' = 0, \tag{75}$$

where $r = 1, 2, 3$, and

$$\begin{aligned} Q_{11}' &= \frac{\rho'}{\rho}\Omega^2 - \bar{c}_{11}' X^2 - \bar{c}_{66}' Y'^2, \\ Q_{22}' &= \frac{\rho'}{\rho}\Omega^2 - \bar{c}_{66}' X^2 - \bar{c}_{22}' Y'^2, \\ Q_{33}' &= \frac{\rho'}{\rho}\Omega^2 - \bar{c}_{55}' X^2 - \bar{c}_{44}' Y'^2, \\ Q_{12}' &= Q_{21}' = (\bar{c}_{12}' + \bar{c}_{66}') XY', \\ Q_{13}' &= Q_{31}' = Q_{23}' = Q_{32}' = 0, \end{aligned} \tag{76}$$

and

$$Y' = \frac{2}{\pi}\eta' b_q, \quad \bar{c}_{pq}' = \frac{c_{pq}'}{c_{66}}. \tag{77}$$

The vanishing of the determinant

$$\det[Q_{rs}'(\Omega, X, Y')] = 0, \tag{78}$$

gives a third-order polynomial equation of $Y'^2$. For given frequency $\Omega$ and wave number $X$, (78) yields three roots, $Y_s'$ or $\eta_s'$, $s = 1, 2, 3$. Thus, the general solution for the displacement in the electrodes are:

$$\begin{aligned} u_1 &= \sum_{s=1}^{3} \alpha_{1s}' \left[A_s' \sin(\eta_s' x_2) \pm B_s' \cos(\eta_s' x_2)\right] e^{i(\xi x_1 - \omega t)}, \\ u_2 &= i \sum_{s=1}^{3} \alpha_{2s}' \left[A_s' \cos(\eta_s' x_2) \mp B_s' \sin(\eta_s' x_2)\right] e^{i(\xi x_1 - \omega t)}, \\ u_3 &= i \sum_{s=1}^{3} \alpha_{3s}' \left[A_s' \cos(\eta_s' x_2) \mp B_s' \sin(\eta_s' x_2)\right] e^{i(\xi x_1 - \omega t)}, \end{aligned} \tag{79}$$

where $\alpha'_{ts}$ satisfy:

$$\sum_{t=1}^{3} Q'_{rt}(\Omega, X, Y'_s)\alpha'_{ts} = 0, \quad r, s = 1, 2, 3. \tag{80}$$

The continuity conditions at the interfaces of the quartz and electrodes are

$$\begin{aligned} u_i(x_2 = \pm b_q^+) &= u_i(x_2 = \pm b_q^-), \quad i = 1, 2, 3, \\ T_p(x_2 = \pm b_q^+) &= T_p(x_2 = \pm b_q^-), \quad p = 2, 4, 6, \end{aligned} \tag{81}$$

and the traction-free and shorted-face conditions are

$$\begin{aligned} T_p(x_2 = \pm b) &= 0, \quad p = 2, 4, 6, \\ \phi(x_2 = \pm b_q) &= 0. \end{aligned} \tag{82}$$

Substitution of (73) and (79) into (63) and (64), respectively, and then into (81) and (82) leads to a system of 10 simultaneous algebraic equations, which can be written as

$$\begin{bmatrix} \mathbf{M}^{TA'}(b) & \mathbf{M}^{TB'}(b) & 0 \\ \mathbf{M}^{TA'}(b_q) & \mathbf{M}^{TB'}(b_q) & -\mathbf{M}^{TA}(b_q) \\ -\mathbf{M}^{uA'}(b_q) & -\mathbf{M}^{uB'}(b_q) & \mathbf{M}^{uA}(b_q) \\ 0 & 0 & \mathbf{M}^{\phi A}(b_q) \end{bmatrix} \begin{pmatrix} \mathbf{A}' \\ \mathbf{B}' \\ \mathbf{A} \end{pmatrix} = \mathbf{0}, \tag{83}$$

where $\mathbf{A}'$, $\mathbf{B}'$, and $\mathbf{A}$ are vectors with components $A'_s$, $B'_s$, and $A_j$, respectively, $s = 1, 2, 3$, $j = 1, 2, 3, 4$, and

$$\begin{aligned} M_{1s}^{TA'}(x_2) &= \beta'_{1s}\sin(\eta'_s x_2), \\ M_{1s}^{uA'}(x_2) &= \alpha'_{1s}\sin(\eta'_s x_2), \\ M_{2s}^{TA'}(x_2) &= \beta'_{2s}\sin(\eta'_s x_2), \\ M_{2s}^{uA'}(x_2) &= \alpha'_{2s}\cos(\eta'_s x_2), \\ M_{3s}^{TA'}(x_2) &= \beta'_{3s}\cos(\eta'_s x_2), \\ M_{3s}^{uA'}(x_2) &= \alpha'_{3s}\cos(\eta'_s x_2), \\ M_{1s}^{TB'}(x_2) &= \beta'_{1s}\cos(\eta'_s x_2), \\ M_{1s}^{uB'}(x_2) &= \alpha'_{1s}\cos(\eta'_s x_2), \\ M_{2s}^{TB'}(x_2) &= \beta'_{2s}\cos(\eta'_s x_2), \\ M_{2s}^{uB'}(x_2) &= -\alpha'_{2s}\sin(\eta'_s x_2), \\ M_{3s}^{TB'}(x_2) &= -\beta'_{3s}\sin(\eta'_s x_2), \\ M_{3s}^{uB'}(x_2) &= -\alpha'_{3s}\sin(\eta'_s x_2), \\ M_{1j}^{TA}(x_2) &= \beta_{1j}\sin(\eta_j x_2), \\ M_{1j}^{uA}(x_2) &= \alpha_{1j}\sin(\eta_j x_2), \\ M_{2j}^{TA}(x_2) &= \beta_{2j}\sin(\eta_j x_2), \\ M_{2j}^{uA}(x_2) &= \alpha_{2j}\cos(\eta_j x_2), \\ M_{3j}^{TA}(x_2) &= \beta_{3j}\cos(\eta_j x_2), \\ M_{3j}^{uA}(x_2) &= \alpha_{3j}\cos(\eta_j x_2), \\ M_{1j}^{\phi A}(x_2) &= \alpha_{4j}\sin(\eta_j x_2), \end{aligned} \tag{84}$$

and

$$\begin{aligned} \beta'_{1s} &= \bar{c}'_{21}\alpha'_{1s}X - \bar{c}'_{22}\alpha'_{2s}Y'_s, \\ \beta'_{2s} &= -\bar{c}'_{44}\alpha'_{3s}Y'_s, \\ \beta'_{3s} &= \bar{c}'_{66}\alpha'_{1s}Y'_s - \alpha'_{2s}X), \\ \beta_{1j} &= \bar{c}_{21}\alpha_{1j}X - \bar{c}_{22}\alpha_{2j}Y_j - \bar{c}_{24}\alpha_{3j}Y_j + \bar{e}_{12}\alpha_{4j}X, \\ \beta_{2j} &= \bar{c}_{41}\alpha_{1j}X - \bar{c}_{42}\alpha_{2j}Y_j - \bar{c}_{44}\alpha_{3j}Y_j + \bar{e}_{14}\alpha_{4j}X, \\ \beta_{3j} &= \bar{c}_{66}(\alpha_{1j}Y_j - \alpha_{2j}X) - \bar{c}_{65}\alpha_{3j}X + \bar{e}_{26}\alpha_{4j}Y_j. \end{aligned} \tag{85}$$

The vanishing of the determinant of the coefficient matrix in (83) gives the dispersion relations of the antisymmetric waves in an infinite plate of AT-cut quartz with two identical electrodes:

$$\mathcal{D}(\Omega, X) = 0. \tag{86}$$

For simple thickness modes (i.e., $u_i$ and $\phi$ are functions of $x_2$ and $t$ only), the governing equations for $u_1$ and $\phi$ are uncoupled from $u_2$ and $u_3$ in (65) and (66), from which the frequency equation for antisymmetric simple thickness-shear modes is obtained:

$$\begin{aligned} &\left[\left(1 + \bar{e}_{26}^2\right)\zeta b_q \cos(\zeta b_q) - \bar{e}_{26}^2 \sin(\zeta b_q)\right]\cos(2\zeta' b_e) \\ &\quad - \bar{c}'_{66}\zeta' b_q \sin(\zeta b_q)\sin(2\zeta' b_e) = 0, \end{aligned} \tag{87}$$

where

$$\zeta = \omega\sqrt{\frac{\rho}{c_{66}(1 + \bar{e}_{26}^2)}}, \quad \zeta' = \omega\sqrt{\frac{\rho'}{\bar{c}'_{66}}}. \tag{88}$$

We note that (87) reduces to:

$$(1 + \bar{e}_{26}^2)\zeta b_q \cos(\zeta b_q) - \bar{e}_{26}^2 \sin(\zeta b_q) = 0, \tag{89}$$

for plates without electrodes ($b_e = 0$), and furthermore to:

$$\cos\left(\omega b_q\sqrt{\frac{\rho}{c_{66}}}\right) = 0, \tag{90}$$

for plates without piezoelectric effect ($e_{26} = 0$). The lowest frequency from (90) is:

$$\omega_1 = \frac{\pi}{2b_q}\sqrt{\frac{c_{66}}{\rho}}, \tag{91}$$

which is the cut-off frequency used for normalization in (49).

## References


[1] R. D. Mindlin, "High frequency vibrations of plated, crystal plates," in *Progress in Applied Mechanics*. The Prager Anniversary Volume. New York: Macmillan, 1963, pp. 73–84.

[2] P. C. Y. Lee, S. Syngellakis, and J. P. Hou, "A two-dimensional theory for high-frequency vibrations of piezoelectric crystal plates with or without electrodes," *J. Appl. Phys.*, vol. 61, no. 4, pp. 1249–1262, 1987.

[3] Q. X. Su, P. B. Kirby, E. Komuro, and R. W. Whatmore, "Edge supported ZnO thin film bulk acoustic wave resonators and filter design," in *Proc. IEEE Int. Freq. Contr. Symp.*, 2000, pp. 434–440.

[4] P. C. Y. Lee and N. Chang, "Harmonic waves in elastic sandwich plates," *J. Elasticity*, vol. 9, no. 1, pp. 51–69, 1979.
[5] J. T. Stewart and Y. K. Yong, "Exact analysis of the propagation of acoustic waves in multilayered anisotropic piezoelectric plates," in *Proc. IEEE Int. Freq. Contr. Symp.*, 1993, pp. 476–501.
[6] P. C. Y. Lee and J. D. Yu, "Governing equations for a piezoelectric plate with graded properties across the thickness," *IEEE Trans. Ultrason., Ferroelect., Freq. Contr.*, vol. 45, no. 1, pp. 236–250, 1998.
[7] P. C. Y. Lee, J. D. Yu, and W. S. Lin, "A new two-dimensional theory for vibrations of piezoelectric crystal plates with electroded faces," *J. Appl. Phys.*, vol. 83, no. 3, pp. 1213–1223, 1998.
[8] Y. K. Yong, J. T. Stewart, and A. Ballato, "A laminated plate theory for high frequency, piezoelectric thin-film resonators," *J. Appl. Phys.*, vol. 74, no. 5, pp. 3028–3046, 1993.
[9] H. F. Tiersten, *Linear Piezoelectric Plate Vibrations*. New York: Plenum, 1969.
[10] P. C. Y. Lee, J. D. Yu, X. Li, and W.-H. Shih, "Piezoelectric ceramic disks with thickness-graded material properties," *IEEE Trans. Ultrason., Ferroelect., Freq. Contr.*, vol. 46, no. 1, pp. 205–215, 1999.
[11] P. C. Y. Lee, R. Huang, X. Li, and W.-H. Shih, "Vibrations and static responses of asymmetric bimorph disks of piezoelectric ceramics," *IEEE Trans. Ultrason., Ferroelect., Freq. Contr.*, vol. 47, no. 3, pp. 706–715, 2000.
[12] P. C. Y. Lee, private notes, unpublished.
[13] I. Koga and H. Fukuyo, "Vibrations of thin piezoelectric quartz plates," *J. Inst. Elec. Commun. Eng. Japan*, vol. 36, no. 2, pp. 59–67, 1953.
[14] R. Bechmann, "Elastic and piezoelectric constants of Alpha-quartz," *Phys. Rev.*, vol. 110, no. 5, p. 1060, 1958.
[15] B. A. Auld, *Acoustic Fields and Waves in Solids*, vol. I. New York: Wiley, 1973.

**Rui Huang** received his B.S. and M.Eng. degrees in mechanics and mechanical engineering from the University of Science and Technology of China (USTC) in 1994 and 1996, respectively, and his Ph.D. degree in civil and environmental engineering from Princeton University in 2001. He is now a research associate at the Civil and Environmental Engineering Department and Princeton Materials Institute of Princeton University.

Dr. Huang's research interests include high-frequency vibrations of piezoelectric crystal plates, smart materials and structures, evolving material structures of small feature sizes, thin films, and other micro/nano-structures.